SERI/PR/9296-T1
(DE81026219)
Distribution Category UC-63

CADMIUM SULFIDE / COPPER SULFIDE HETEROJUNCTION CELL RESEARCH BY SPUTTER DEPOSITION

Quarterly Technical Progress Report

Period: December 1, 1980 - February 28, 1981

By

John A. Thornton
Telic Corporation
1631 Colorado Avenue
Santa Monica, California 90404

W. W. Anderson
Lockheed Palo Alto Research Laboratory
Palo Alto, California 94304

and

John D. Meakin
University of Delaware
Institute of Energy Conversion
Newark, Delaware 19711

April 3, 1981

Work Performed Under Contract No. XW-Ø-9296

Solar Energy Research Institute
1536 Cole Boulevard
Golden, Colorado 80401

Blank Page

TABLE OF CONTENTS

ABSTRACT Page

1. PROJECT DESCRIPTION..... 1
   1.1 Overall Objective..... 1
   1.2 Work Statement..... 1

2. SHORT CIRCUIT CURRENT..... 3
   2.1 Introduction..... 3
   2.2 Photoluminescence Studies..... 4
   2.3 All-Sputter Deposited Cells..... 10

3. OPTIMIZATION OF Cu_2S DEPOSITION..... 13
   3.1 Investigation of Cu_2S Deposition..... 13
   3.2 Hybrid Cell Fabrication, Sputtered Cu_2S/Evaporated CdS..... 16

4. IMPROVED DEVICE DESIGN..... 24

5. PLANAR MAGNETRON SPUTTERING..... 27

6. DEVICE CHARACTERIZATION AND FABRICATION..... 33

7. SUMMARY STATUS..... 35

REFERENCES

APPENDIX A
   Analysis of Dispersion in Measured Capacitance of CdS/Cu_2S Solar Cells, by W. W. Anderson

LIST OF FIGURES AND TABLES

Page

FIG. 1. General configuration of all-sputter-deposited solar cells..... 5

FIG. 2. Photoluminescence intensity spectrum for sputtered and evaporated CdS films..... 8

FIG. 3. Photoluminescence intensity spectrum for sputtered film that was heat treated in sputtered Cd flux, compared with evaporated film..... 9

FIG. 4. Schematic illustration of multi-source deposition apparatus..... 11

FIG. 5. Resistivity of copper sulfide coatings formed by reactive sputtering Cu in Ar & H_2S..... 15

FIG. 6. Cathode and wall surface conditioning while reactive sputtering Cu in Ar & H_2S at various H_2S injection rates..... 17

TABLE I Results of laser scan evaluation of uniformity of sputtered Cu_2S layers on hybrid (sputtered Cu_2S/evaporated CdS) cells..... 19

TABLE II Photovoltaic performance of hybrid (sputtered Cu_2S/evaporated CdS) cells given heat treatments at IEC..... 20

FIG. 7. I-V characteristics for hybrid (sputtered-Cu_2S/evaporated CdS) cells deposited at different substrate temperatures..... 22

FIG. 8. I-V characteristics for hybrid (sputtered-Cu_2S/evaporated CdS) cells having Cu_2S layers of different thicknesses..... 23

TABLE III Performance of second series of hybrid (sputtered Cu_2S/ evaporated CdS) cells given heat treatments at Lockheed..... 25

FIG. 9. Spectral response of short circuit current in hybrid (sputtered Cu_2S/evaporated CdS) cells having Cu_2S layers of different thicknesses..... 26

FIG.10. Deposition rate versus H_2S injection rate for reactive sputtered CdS deposited using planar magnetron sputtering source..... 28

FIG.11. Deposition rate versus substrate temperature for reactive sputtered CdS deposited using planar magnetron sputtering source..... 31

LIST OF FIGURES AND TABLES

Page

FIG.12 Resistivity versus H_2S injection rate for reactively sputtered CdS deposited using planar magnetron sputtering source..... 32

FIG.13 Resistivity versus substrate temperature for reactive sputtered CdS deposited using planar magnetron sputtering source..... 34

ABSTRACT

This report covers work conducted during the period December 1, 1980, through February 28, 1981.

Significant progress has been made on all of the research tasks. Photoluminescence spectral measurements on 6000 nm thick reactive sputtered CdS coatings have yielded exciton and "green edge emission" spectra which are similar in their general character to those recorded from the evaporated CdS that yields high performance cells. The photoluminescence spectra of the sputtered coatings will be correlated with the performance of these materials when used for cells.

All-sputter-deposited cells with composite doped and undoped CdS layers have yielded $J_{sc} \sim 3$ mA/cm^2. This is the highest J_{sc} that has been achieved for cells with this structure, which is designed to increase the junction electric field.

A hybrid cell with sputtered Cu_2S deposited onto evaporated CdS supplied by IEC has yielded $J_{sc} \sim 18$ mA/cm^2 (under illumination of 87.5 mW/cm^2), V_{oc} 0.47V, FF = 0.60, and $\eta = 5.74\%$ with no AR coating.

Cu_2S reactive sputtering experiments have further elucidated the influence of cathode and wall conditioning on the deposition process. CdS reactive sputtering experiments using a planar magnetron source have been initiated. Data are reported on the dependence of the deposition rate and coating resistivity on the substrate temperature and H_2S injection rate. The planar magnetron data are generally consistent with data previously reported for CdS reactive sputtering using cylindrical-post magnetrons. The resistivities of CdS coatings deposited using the planar magnetron are typically a factor of from three to ten lower than for coatings deposited using the cylindrical magnetrons.

An analysis is reported which relates the frequency dispersion observed in C-V measurements on CdS/Cu_2S solar cells to the surface resistivity of the Cu_2S layer.

1. PROJECT DESCRIPTION

1.1 Overall Objective

The overall objective of the program is to investigate and evaluate the application of magnetron reactive sputtering for the production of solar cell quality thin films of CdS/Cu_2S.

Sputtering, particularly using magnetron methods, has great promise for depositing high quality films over large areas at the production volumes required to reach the long term national goals of \$0.15-0.40/peak-watt for thin film photovoltaic modules. A general goal is to find the proper role for sputtering technology in the overall photovoltaic program.

The all-sputter-deposited thin film CdS/Cu_2S solar cells fabricated thus-far have been characterized by low short circuit currents, and efficiencies of about 1% or less.[1,2] A specific objective is to increase the short circuit current and improve the efficiency of these devices.[1] Particular attention is being given to identifying differences between sputtered and evaporated coatings and heterojunctions, and to determining the physical basis for these differences. Accordingly, liberal use is being made of hybrid cells which incorporate various combinations of sputtered and conventionally formed layers (i.e., layers of evaporated CdS and wet and dry CuCl ion exchange-formed Cu_2S).

A three-laboratory team has been assembled to conduct the program.[1] The reactive sputtering process is being investigated, and the sputtered coatings and cells are being prepared, at Telic Corporation. Characterization of the cells and coatings is being done at the Lockheed Palo Alto Research Laboratory. Evaporated CdS coatings for hybrid cells and comparative studies, and wet and dry ion exchange Cu_2S layers for the hybrid cells, are being prepared at the University of Delaware Institute of Energy Conversion. Cell performance losses are also being analyzed at IEC. The program is being coordinated by Telic Corporation.

1.2 Work Statement

The present program was formulated to address the deficiencies in the all-sputter-deposited cells, which were identified in previous work and are reviewed in Ref. 1. The basic tasks are described below.

Task 1 - INCREASE SHORT CIRCUIT CURRENT

This task involves examining the effectiveness of various procedures for increasing the short circuit current. The procedures to be tried will include (1) using graded doping concentrations in CdS films; (2) using uniform CdS films with improved properties and conductivity control by doping and off-stoichiometric deposition; (3) etching of CdS surface in HCl prior to Cu_2S deposition; (4) using post-deposition in situ heat treatments of CdS films prior to Cu_2S deposition; (5) using post-deposition in situ heat treatments of CdS/Cu_2S heterojunctions; (6) forming hybrid cells by depositing Cu_2S onto sputtered CdS using the ion exchange processes; and (7) using techniques such as photoluminescence and scanning electron microscopy to evaluate and compare sputter-deposition and evaporated CdS.

A second quarter goal is to achieve short circuit currents of 10 mA/cm^2 or greater.

Task 2 - OPTIMIZE Cu_2S DEPOSITION

This task involves attempting to establish optimum conditions for the Cu_2S deposition. Attention will be given to determining the optimum thickness for the Cu_2S. This task will be performed in conjunction with Task 1 to achieve efficient solar cells. Particular attention will be given to comparing and contrasting the characteristics of Cu_2S produced by sputtering and by the ion exchange methods.

Task 3 - IMPROVE DEVICE DESIGN

This task involves making improvements in the basic device design. It will be undertaken once short circuit currents >10 mA/cm^2, as specified in Task 1, have been achieved. The task will include examining the effects of better top grid electrodes and antireflection coatings. Quantitative photon economy analysis will be made to evaluate improvements and to identify approaches for achieving further improvements.

Task 4 - PLANAR MAGNETRON SPUTTERING

This task involves examining the ability of a planar magnetron sputtering source to produce CdS films of high conductivity by off-stoichiometry doping.

Task 5 - DEVICE CHARACTERIZATION AND FABRICATION

This task will be conducted in support of the other tasks described above. It will involve characterizing device performance and determining the effectiveness of various post-deposition treatments. The effects of heat treatment on the photovoltaic properties of the cells will be investigated. The heat treatments will be conducted in H_2/Ar and in air. The cells will be characterized prior to, and progressively through the course of the heat treatments. The cells will be characterized by the following techniques:

1) I-V characterization of solar cells will be made in dark and under AM1 illumination.
2) C-V characterization of the cells will be made in dark, AM1 illumination, and as a function of the spectral content of the light. The relationship between photo-capacitance and junction collection efficiency will be determined.
3) The effects of heat treatment on the dark capacitance and photo-capacitance will be determined.
4) The quantum efficiency of selected cells will be determined as a function of wavelength, both with and without bias light.

The optimum conditions for producing high efficiency CdS/Cu_2S solar cells by sputtering will be determined. The optimization will include the following:

1) Determining the effects of the Cu_2S thickness on J_{sc} and cell performance;
2) Determining the effects of graded doping profiles on cell performance;
3) Determining the effects on cell performance of <u>in situ</u> heat treatment of the CdS layer prior to Cu_2S deposition;
4) Determining the effects on cell performance of etching the CdS prior to the Cu_2S deposition.

Hybrid cells will be fabricated and tested as a means of evaluating the performance of the various sputtered layers required to make a cell. This activity will include:

1) Fabrication and testing of hybrid cells in which Cu_2S is deposited by sputtering onto evaporated CdS that has been demonstrated to be capable of producing conventional cells with efficiencies of over 7.5%.
2) Fabrication and testing of hybrid cells which incorporate sputter-deposited CdS and Cu_2S layers formed by both the wet and dry CuCl ion exchange method.

2. SHORT CIRCUIT CURRENT (Task 1)

2.1 <u>Introduction</u>

The major deficiency in the all-sputter-deposited cells fabricated in our previous work was a low short circuit current (J_{sc}).[1,2] The cell I-V characteristics indicated that the cause of the low J_{sc} was excessive junction recombination losses. Capacitance-voltage measurements suggested that the recombination losses were due primarily to a low junction electric field, which resulted in turn from the fact that the depletion layer in the sputter-deposited films did not shrink significantly under AM1 illumination. Thus it was concluded that the poor performance of the sputter-deposited cells can be traced

primarily to the properties of the CdS layer.[2]

Accordingly, the approach on the present program for increasing the short circuit current is to increase the junction electric field by modifying the properties of the sputtered CdS and/or the configuration of the junction. The particular approaches fall into three general categories.

1) The use of special tests and hybrid cell fabrication to further elucidate the differences between sputtered CdS coatings deposited under various conditions and the evaporated CdS that yields high performance cells.

2) The use of special post-deposition heat treatments of the sputtered CdS to reduce the resistivity and improve the crystallographic perfection.

3) The fabrication of cells with composite, doped and undoped, CdS layers, of the type shown in Fig. 1, which are configured to place a strong electric field at the junction.

The work conducted this quarter on Task 1 has involved primarily (1) photoluminescence studies of sputter-deposited CdS, and (2) the fabrication of several types of all-sputter-deposited cells.

2.2 Photoluminescence Studies

The CdS photoluminescence spectra has been characterized as consisting of two features.[3] One feature consists of a relatively sharp group of lines, involving exciton transitions, and has been termed the "blue edge emission". Bound exciton transitions have been identified which involve (1) an exciton bound to a neutral acceptor, (2) an exciton bound to a neutral donor, and (3) an exciton bound to an ionized donor.

The second feature consists of a broad multi-line spectra involving defects, and has been termed the "green edge emission". Each transition gives rise to a band consisting of a set of lines associated with the zeroth order and phonon-assisted transitions between a pair of levels. Thus the presence of multiple levels and/or an elevated temperature (e.g., 77°K versus 4.2°K) can make the emission appear as a broad continuous band. The green emission has been found to be sensitive to variations in the crystal defect chemistry--i.e., to heat treatments in cadmium and sulfur vapor--and therefore to be sensitive to native defects. However, the exact nature of the defect or

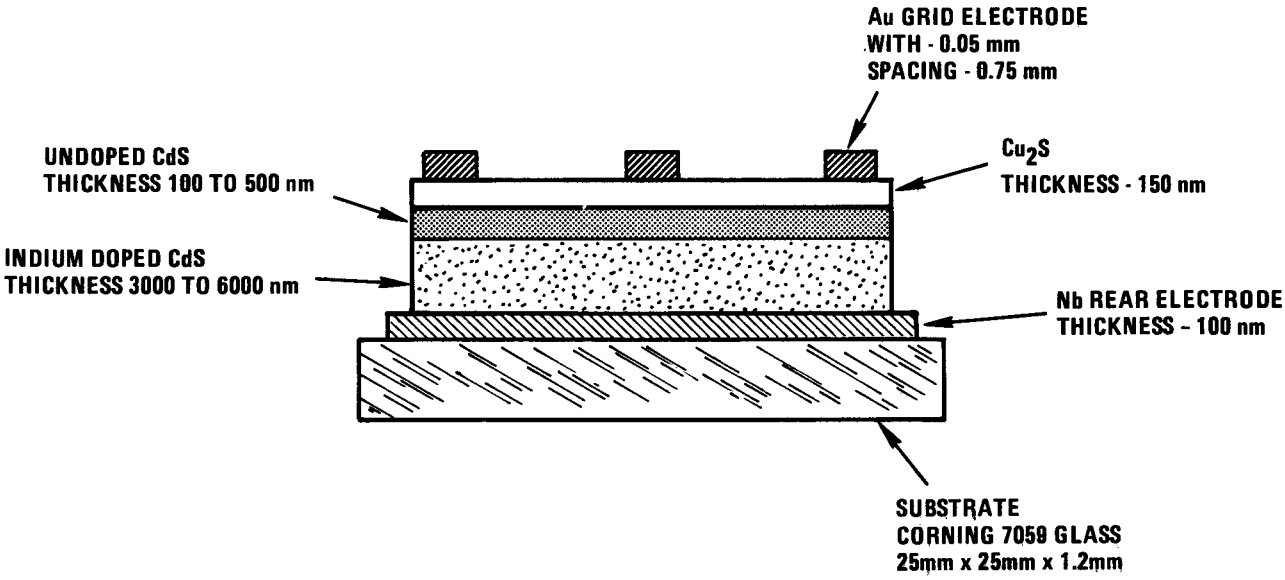

FIG. 1 General configuration of all-sputter-deposited solar cells.

defects producing the emission remains a matter of debate.[3]

Christmann, et al.,[4] studied the structure and edge emission from evaporated CdS films grown epitaxially on SrF_2 substrates. Their work appears to be relevant to our observations and will be reviewed briefly. Coatings grown at low supersaturations exhibited a smooth surface, and an edge emission at 4.2°K that consisted of a broad "green emission" continuum centered at about 530 nm with no exciton lines. The films were concluded to have a large excess of Cd in solution, and Cd interstitials were concluded to provide the defect level responsible for the broad-band emission.

Coatings grown under medium supersaturation exhibited a green emission line spectrum ranging from 518 to 552 nm and weak exciton lines at about 490 nm.[3] The coatings were concluded to contain less Cd than the low-supersaturation coatings described above. The green emission series was concluded to be produced by an electron bound to a donor recombining with a hole bound to an acceptor.

Coatings grown under high supersaturation exhibited a green emission line spectra ranging from 514 to 549 nm with strong exciton lines at 487 and 489 nm. These coatings were concluded to contain a second phase of elemental Cd, but with the CdS containing even less Cd in solution than the medium-supersaturating coatings described above. The green emission lines were attributed to a free electron recombining with a hole bound to an acceptor.

In studies at IEC it has been found that an empirical correlation exists between cell performance and the photoluminescence spectra of the CdS.[5] Therefore the photoluminescence spectra of sputter deposited CdS coatings are being evaluated. Preliminary results were reported in Ref. 1. It was found that relatively thin (3000 nm thick) sputtered coatings of pure CdS, deposited at a substrate temperature of 250°C under conditions typical of those which had been used in cell fabrication, did not exhibit exciton or green edge emission, although a long wavelength band in the 700-800 nm region was observed. Thicker (6000 nm) CdS layers prepared under various deposition conditions exhibited visible evidence of a yellow photoluminescence. Emission was not seen for

6000 nm thick coatings that were doped with 0.1 at. percent of indium.

Spectral data are now available for the 6000 nm thick coatings, with the yellow emission, which are described above. Figure 2 shows the spectrum for a sputtered coating deposited at 250°C onto Nb-metallized 7059 glass. The coating resistivity was about $10^4 \Omega$-cm. The spectrum of a 5000 nm thick evaporated coating, which was deposited directly onto 7059 glass at IEC, is shown for comparison. The radiation intensities for the two coatings are relative values and cannot be compared directly. Note, however, that the exciton line is relatively weak in the sputtered film. This is consistent with the Christmann, et al., observations described above, since the relatively low deposition rate (~1 nm/s) in the sputtering case, along with the substrate temperature of 250°C, corresponds to a small degree of supersaturation.

Figure 3 shows the spectrum of a sputtered coating which was deposited under the same conditions as the coating shown in Fig. 2, but was then cooled in a sputtered flux of elemental Cd to a temperature of 150°C, as described in Ref. 1 (Section 2.3). This treatment reduced the coating resistivity to about $10^2 \Omega$-cm. Note that the exciton line is virtually absent. This is also consistent with Christmann, et al.'s observations that a large excess of Cd in CdS suppressed the exciton emission. Halsted[3] reports cases where prolonged heat treatment in Cd vapor eliminated both the exciton and green emissions.

The peak of the edge emission band spectrum for the sputtered coatings is seen to be at about 540-542 nm as compared to about 522 nm for the evaporated coatings. The general direction of the shift is again consistent with Christmann, who observed that low supersaturation and a high in-solution Cd content shifted the broad emission from 520 to 530 nm. Internal stress is an additional factor which can cause wavelength shifts.[4]

In more recent work thin (3000 nm) CdS coatings deposited at relatively high rates (~3 nm/s) using a planar magnetron (see Section 5) were found to be visually photoluminescent, with an emission having a more green appearance than that of the coatings shown in Figs. 1 and 2. Sample coatings are being

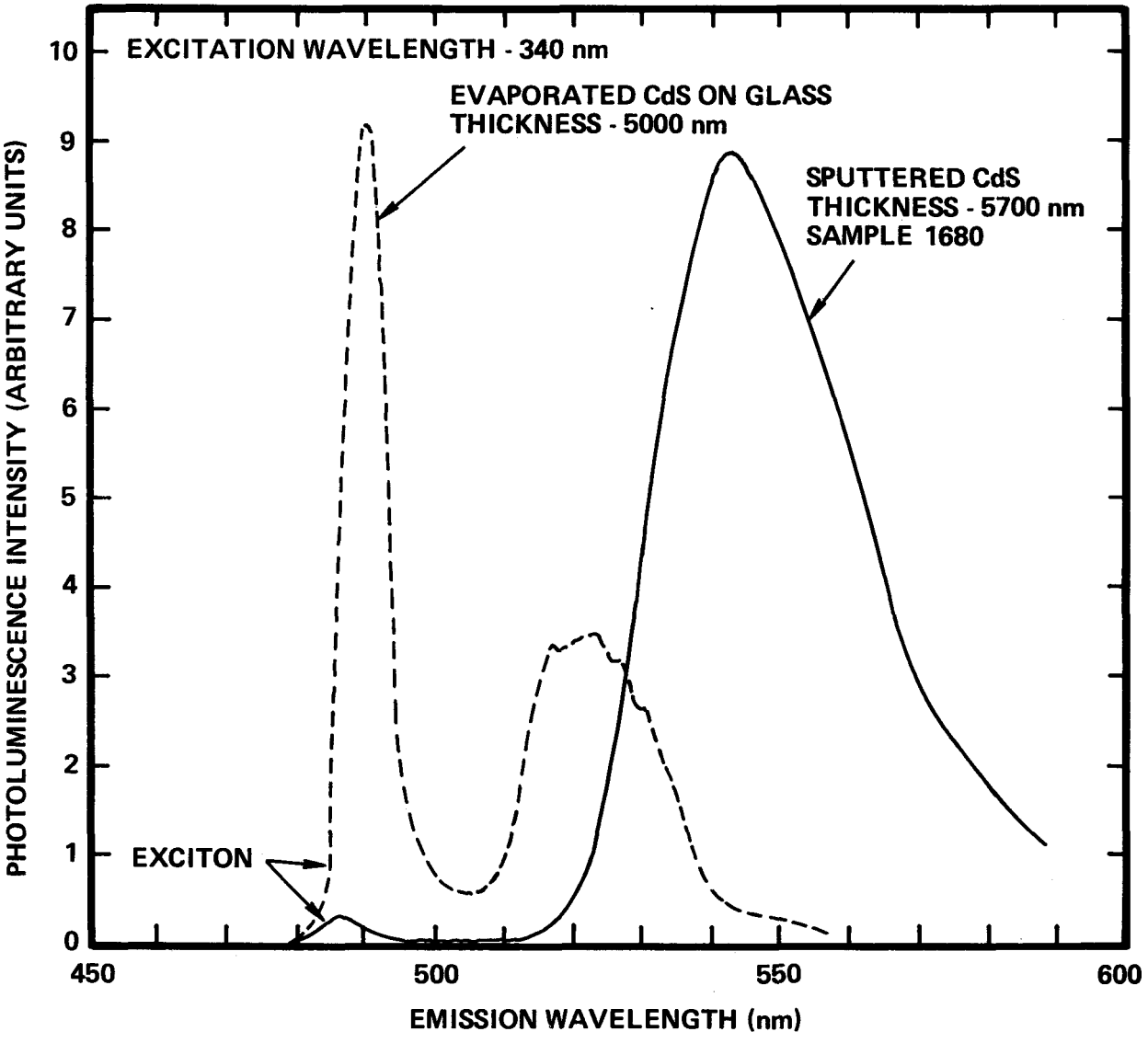

FIG. 2 Photoluminescence intensity spectrum for sputtered and evaporated CdS films. Reactive sputtered film deposited on Nb coated glass substrate at 250°C using H_2S injection rate of 57 Pa-liters/sec. Evaporated coating prepared at IEC.

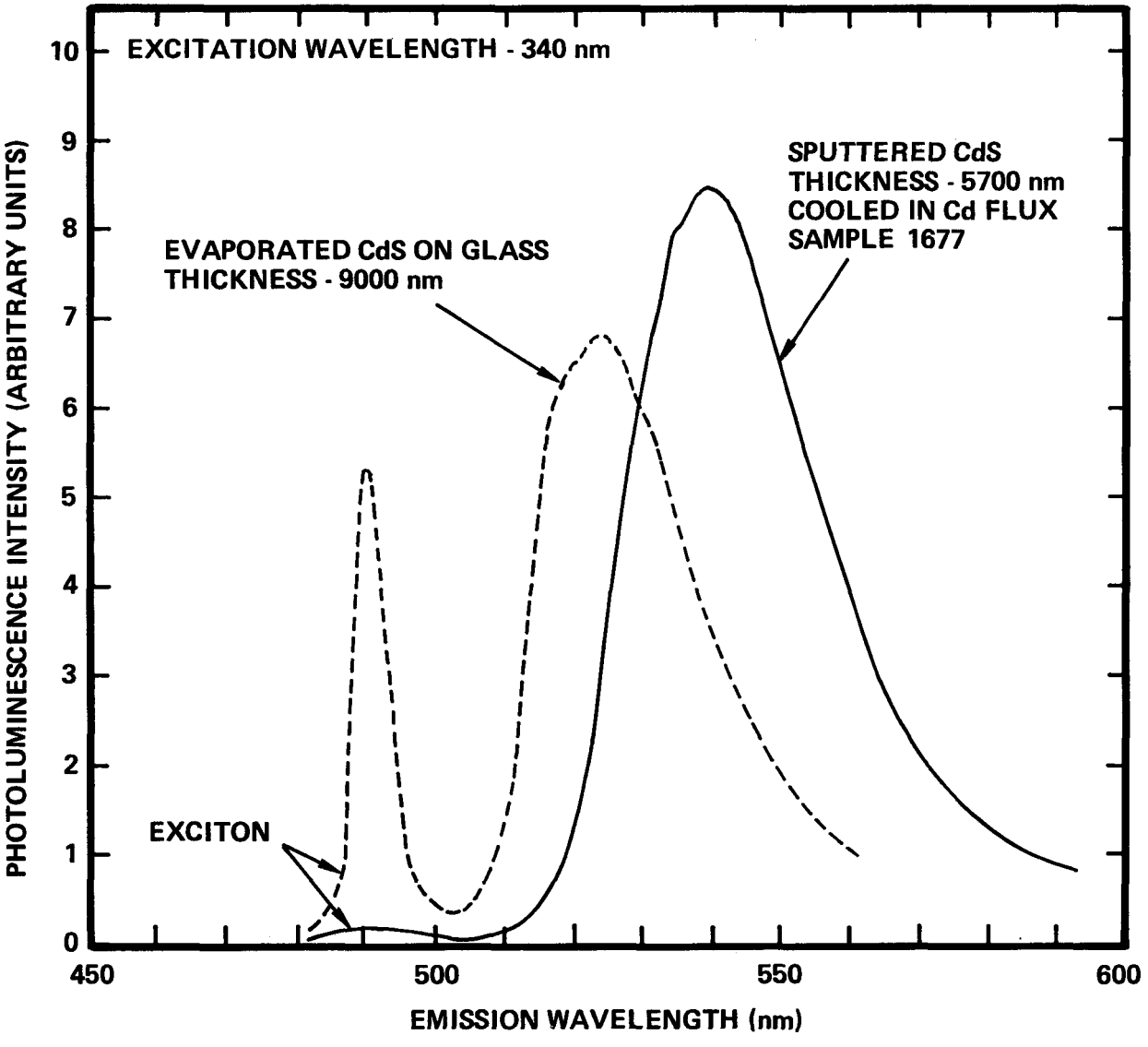

FIG. 3 Photoluminescence intensity spectrum for sputtered coating that was deposited under same conditions as coating shown in Fig. 2 and then cooled in sputtered flux of elemental Cd to temperature of 150°C as described in Ref. 1. Evaporated coating prepared at IEC shown for comparison.

sent to IEC for spectral analysis.

The achievement of visible photoluminescence in cylindrical magnetron sputtered CdS layers 6000 nm thick, but not in layers 3000 nm thick, suggested the possibility that the thin coatings might be affected by material passing out of the substrates. Several experiments were performed to test this hypothesis. The results are summarized below.

1) CdS layers 6000 nm thick on Nb coated glass yielded strong-visible photoluminescence when deposited at a substrate temperature of 250°C, but yielded very little photoluminescence when deposited at 300°C.

2) Thin (3000 nm) sputtered CdS coatings deposited at 250°C onto various substrate materials that might react with the CdS (sputtered-Nb, sputtered-stainless steel, sputtered-brass, bulk-stainless steel and bulk-brass) did not yield visible photoluminescence. In contrast 3000 nm thick sputtered CdS coatings deposited at the same time onto uncoated quartz substrates did yield visible photoluminescence.

3) Thin (3000 nm) CdS coatings, deposited at a relatively low temperature (~200°C) onto glass, precoated with sputtered brass and sputtered stainless steel, did yield visible photoluminescence.

Future studies will attempt to correlate the photoluminescence spectra of the sputtered CdS with cells fabricated from the material.

2.3 All-Sputter Deposited Cells

The all-sputter-deposited cells were fabricated using the multi-source deposition apparatus shown in Fig. 4. The apparatus was configured with Nb, Cd, Cd-0.1 at.% In, and Cu cylindrical-post magnetron sources for these depositions. The design and operation of the apparatus is described in Ref. 2.

The work completed during this reporting period consisted of fabricating a few cells each, for a number of different configurations. The objective was to provide a preliminary survey of several cell configurations that might influence the junction electric field as well as to continue shakedown activities of the multi-source apparatus. Thus the cell configurations differed primarily in the nature of CdS layer. It should be noted that the multi-source apparatus is very versatile in terms of the range of device configurations that can be fabricated.

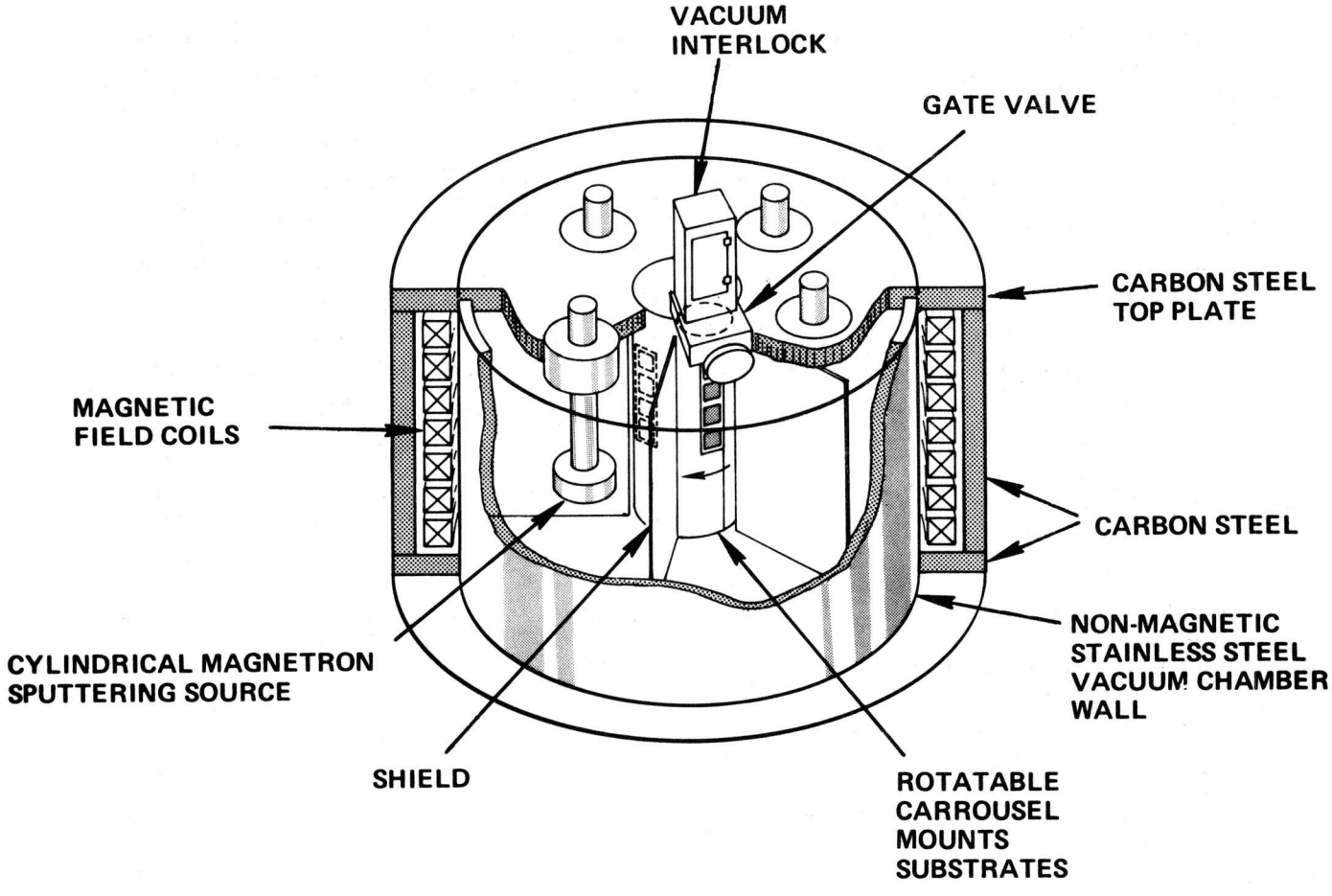

FIG. 4 Schematic illustration of multi-source deposition apparatus.

The general configuration for the all-sputter-deposited cells is shown in Fig. 1. The substrates were 25 mm x 25 mm x 1.2 mm borsilicate (Corning 7059) glass plates. The rear electrode was a 100 nm thick sputter-deposited Nb layer. The reactively sputtered CdS layer was typically 3000 to 5000 nm thick. In some cases it was a single layer. In other cases it was a composite layer consisting of doped and undoped regions, as shown in Fig. 1. The Cu_2S layer was deposited by reactive sputtering without breaking vacuum. It was typically 150 nm thick. The top grid electrode was deposited in a separate chamber by sputtering, using a deposition mask.

Three cells were fabricated during each run. In one run, cells (1894-1896) were fabricated, as a reference, using 5000 nm thick layers of the CdS material that is deposited with a cylindrical-post magnetron under typical conditions (250°C and H_2S injection rate of 57 Pa-liters/sec) when no special effort is made to control the film resistivity.[2] The material has a resistivity of about $10^4 \Omega$-cm (measured in the plane of the film) and will be termed the "basic CdS". (The photoluminescence spectra is shown in Fig. 2.) The devices were characterized by a very high series resistance and reconfirmed the need for a means of resistivity control in the sputtered CdS layers.

Several cells (1790-1792 and 1796-1798) were fabricated with CdS layers deposited using the pulsed H_2S gas injection method for controlling the resistivity. This method has produced CdS resistivities of about $10^3 \Omega$-cm, measured in the plane of the film, and was used in the highest performance all-sputtered cells which were fabricated in our previous work[2] (prior to assembly of the interlock apparatus). However, the cells fabricated during the present series behaved as though the CdS layer was very thin and indicate that additional work will be required if the pulsed-gas injection method is to be scaled for effective use in the larger apparatus presently being used (Fig. 4).

In one run, cells (1790-1792) were fabricated with 4000 nm thick CdS layers in which the resistivity was controlled by cooling in a flux of sputtered Cd, as described in Ref. 1. (The photoluminescence spectra of a similar material is shown in Fig. 3). The junctions yielded ohmic rather than diode behavior

and indicate that a less extreme post-deposition Cd treatment should be used.

In one run, cells (1805-1807) were fabricated with composite CdS layers of the type shown in Fig. 1. The 5700 nm thick base layer was doped with 0.1 at.% In. The layer adjacent to the junction was a 500 nm thick film of "basic CdS". Both layers were deposited at 250°C. The Cu_2S layer was 150 nm thick. It was deposited at 40°C, using an H_2S injection rate of 17 Pa-liters/sec and a cathode current density of 4.7 mA/cm^2. The cells were given heat treatments at Lockheed in Ar-2% H_2 at 150-160°C. The heat treated cells yielded $J_{sc} \sim$ 3 mA/cm^2, $V_{oc} \sim 0.44$V, and FF ~ 0.3, which, although poor, exceed the best performance achieved for a cell with the composite configuration on the previous program (#917, $J_{sc} \sim 2.5$ mA/cm^2, $V_{oc} \sim 0.32$V, FF ~ 0.3)[2]. It should be noted in this respect that the work on cells with this structure is still in a very preliminary stage, with less than ten runs having been made on both programs.

3. OPTIMIZATION OF Cu_2S DEPOSITION

3.1 Investigation of Cu_2S Deposition

Reactions at both the cathode and the chamber wall and substrate surfaces are important in the reactive sputtering process. The time constants for equilibration of these reactions after a change in operating conditions must be taken into account if consistent coating properties are to be achieved. The time constants can differ from one surface to another, and these differences are important in apparatus scaling.

In our previous Cu_xS reactive sputtering work inconsistencies in coating properties were encountered and attributed to long equilibration times for the cathode and/or chamber wall surfaces.[6] An important aspect of the cathode and wall conditioning problem is the effect of exposing these surfaces to the atmosphere when the vacuum chamber is opened for substrate loading. Avoiding this exposure was one of the primary reasons for incorporating the vacuum interlock into the apparatus (see Fig. 4) which is being used in the present program. By removing the atmospheric exposure effects, the vacuum interlock

permits experiments to be conducted which are designed to assist in identifying the individual effects of the cathode and the wall surface on the process equilibration.

Accordingly, a series of experiments is being performed in which the Cu_xS reactive sputtering equilibration times, as manifested by the discharge voltage and coating resistivity, are being examined under various initial cathode and wall conditions selected to expose the relative effects of these surfaces. Other deposition conditions such as the current density and H_2S injection rate are being kept constant. The initial cathode and wall conditions are as follows.

1) Both cathode and wall surfaces in "clean Cu state" formed by sputter-removing surface layers from the cathode and depositing elemental Cu on the walls.
2) Cathode surface in clean Cu state. Wall surfaces in "conditioned-state" formed by extended operation at the operating conditions (cathode current density and H_2S injection rate) in question.
3) Cathode surface in conditioned-state and wall surface in clean Cu state formed by the deposition of elemental Cu.

The results of equilibration experiments with the starting condition listed under (1) above were reported in Ref. 1. These data are summarized in Fig. 5B by curve (a). New data for the starting condition listed under (2) are given by curve (b). Figure 5A shows the resistivity versus H_2S injection rate for Cu_xS coatings deposited, under otherwise constant sputtering conditions, in previous work.[7] The data in Fig. 5B were obtained at a constant H_2S injection rate corresponding to point (x) in Fig. 5A. Note that as the wall reactivity varies during conditioning the resistivity variations in curve (a) of Fig. 5B trace out a relationship that is very similar to the one shown in Fig. 5A.[1] The runs were of 15 minutes duration with the substrates introduced through the vacuum interlock. Thus the equilibration time is seen to be about 2 1/2 hrs, which illustrates the difficulties that can be encountered when attempting to deposit consistent coatings without properly conditioned surfaces.

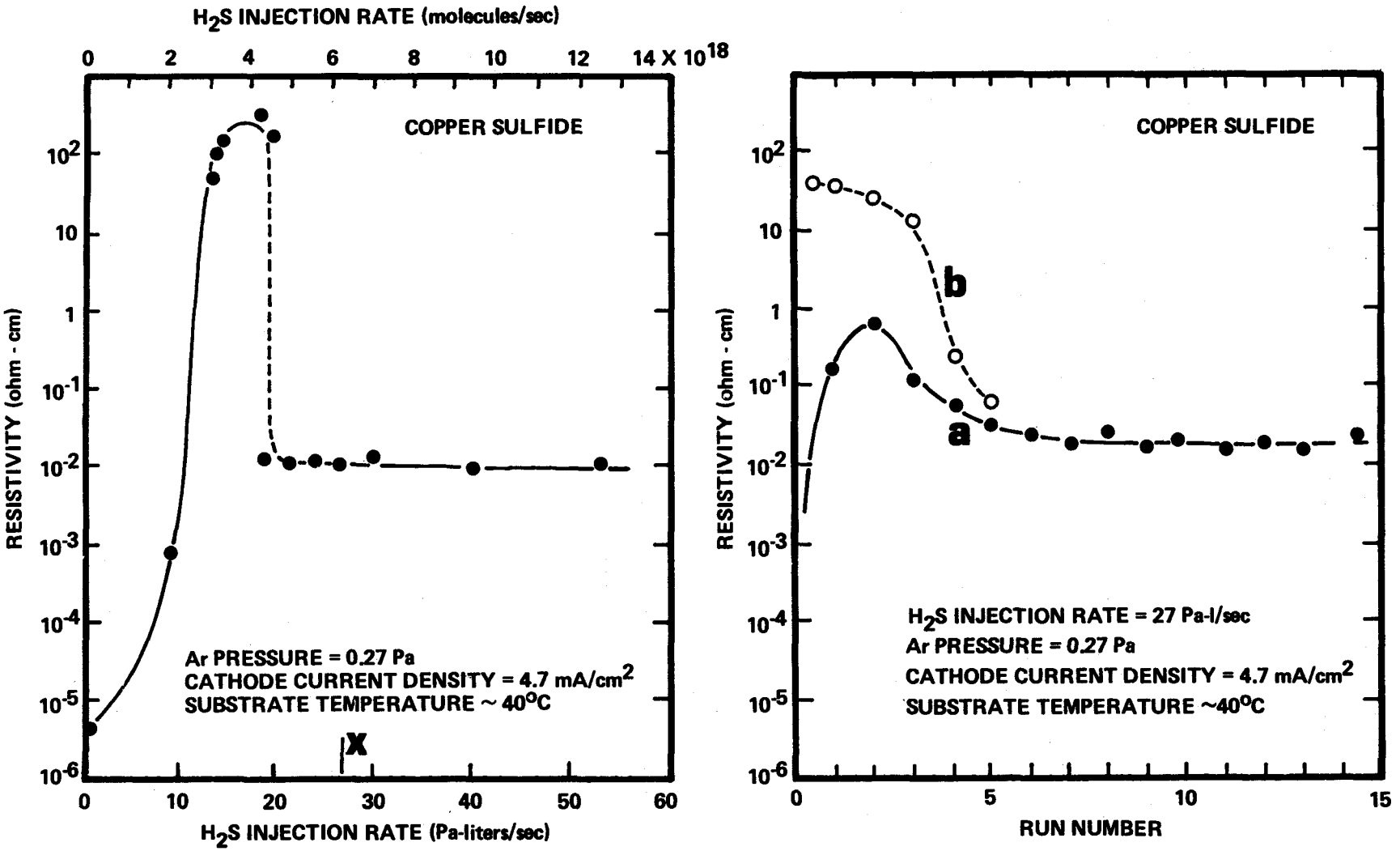

FIG. 5 Resistivity of copper sulfide coatings formed by reactive sputtering Cu in Ar+H_2S. (A) Variation of coating resistivity with H_2S injection rate; data from Ref. 7. (B) Equilibration of operation conditions at fixed H_2S injection rate corresponding to (x) in Fig. 5A and two different initial states for cathode and wall surfaces (see text).

Curve (b) shows the new data for the starting condition of a clean cathode and conditioned walls (condition No. 2, listed above). The data indicate that the cathode places a Cu-rich condition on the walls before becoming conditioned itself, with the result that the overall conditioning time for achieving consistent coatings is again about 2 1/2 hrs for the operating conditions being used.

The data in Fig. 5 imply that consistent Cu_xS reactive sputtering can be achieved, but that care must be taken to reconditioning the surfaces at new operating conditions. Figure 6 shows wall surface conditioning at two H_2S injection rates and a common discharge current density. Curve (a) corresponds to the data given in Fig. 5B. Curve (b) shows the system equilibration at a lower H_2S injection rate. The data for curve (b), as with curve (a), were generated by first sputtering in pure Ar to clean the cathode and deposit fresh Cu on the system walls. In the case of curve (b) the system was operated for 60 min (corresponds to four 15 min runs) at 0.13 Pa or Ar and the H_2S injection rate of interest (17 Pa-liters/sec) before detailed resistivity measurements were commenced. Finally the series of 15 min deposition runs (5 min with substrates shielded followed by 10 min of coating deposition) were made with the substrates introduced through the vacuum interlock. Resistivities were measured by depositing in-situ Nb electrodes. (Consistent results were achieved using Au electrodes). It is seen that the lower injection rate, (curve b) required a longer equilibration time, and appears to have equilibrated the system in a state which produces coatings with a greater resistivity than the data shown by curve (a). These data imply that the resistivity peak in Fig. 5A might have been observed to occur at lower injection rates if sufficient time had been allowed for equilibration.

3.2 Hybrid Cell Fabrication, Sputtered Cu_2S/Evaporated CdS

The fabrication of hybrid cells, which combine sputter deposited Cu_2S with solar cell quality evaporated CdS, permits an evaluation of the sputtered Cu_2S, that is independent of the difficulties that have been encountered with the sputtered CdS.[1] It also permits sputtering to be examined as a deposition

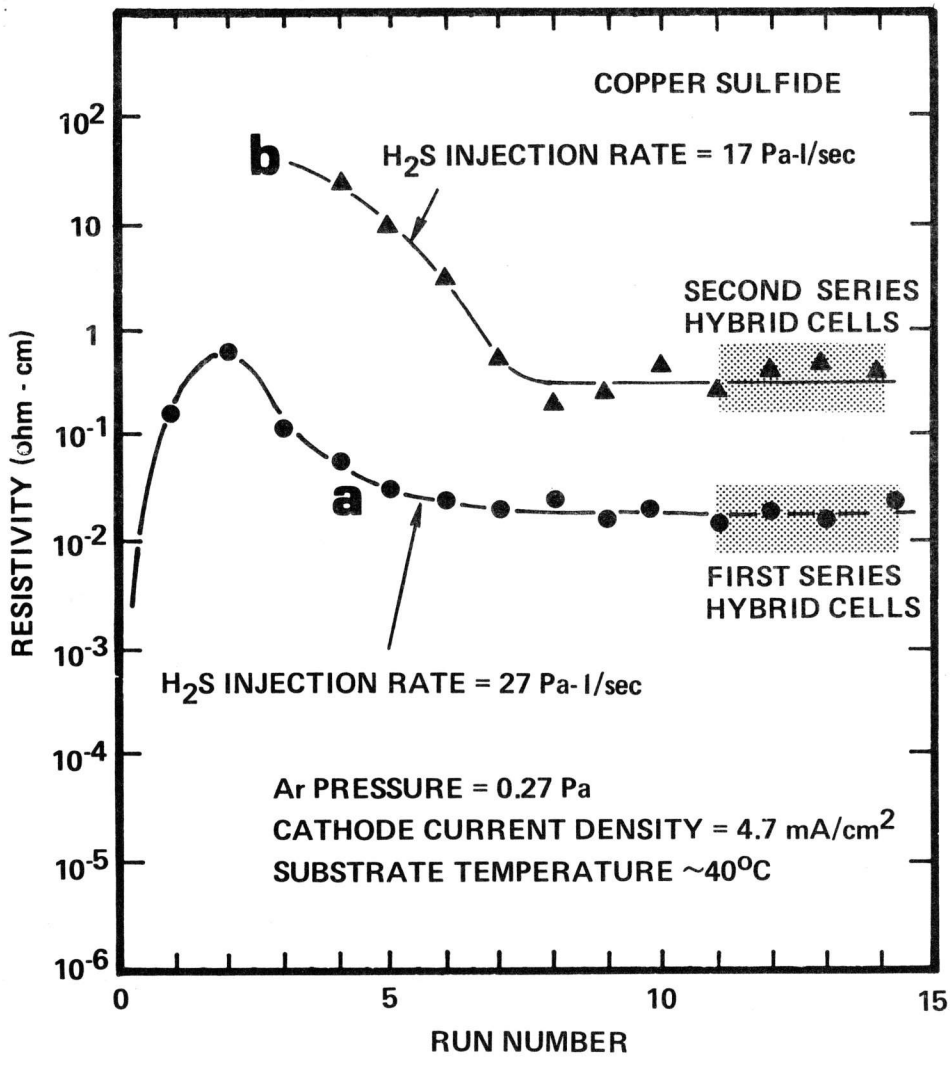

FIG. 6 Resistivity variation during conditioning of cathode and wall surfaces while reactive sputtering Cu in Ar and H_2S at two different H_2S injection rates. Initial cathode surface--fresh sputter-cleaned Cu. Initial wall surface--freshly deposited Cu.

method that could be used in combination with evaporation to provide an all-vacuum cell fabrication process.

Two sets of hybrid cells have been fabricated. One set was deposited with the Cu_xS sputtering system equilibrated along curve (a) in Fig. 6, as indicated by the shaded region. The substrates were 25 mm x 25 mm evaporated CdS coatings on Zn coated 0.03-0.04 mm thick copper sheet. The substrates were supplied by IEC. During each run two CdS substrates and one glass (Corning 7059) reference substrate were coated. The reference coating was used to determine the thickness and resistivity of the Cu_2S. Coatings 75 nm, 150 nm, and 300 nm were deposited at substrate temperatures of 40°C and 120°C. Resistivities were in the range $7x10^{-3}\,\Omega$-cm to $4x10^{-2}\,\Omega$-cm. The details of the deposition procedure and conditions were reported in Ref. 1. One cell from each run was given a Au top grid electrode of the type shown in Fig. 1 and sent to Lockheed. The other heterojunction was sent ungridded to IEC for analysis. The results of the Lockheed heat treatment and cell analysis studies were reported in detail in Ref. 1. The heat treatments were done at 150-155°C in Ar-2% H_2. The thin Cu_2S layers deposited at 40°C yielded the best performance, $J_{sc} \sim 10.2$ mA/cm^2 at 100 mW/cm^2, $V_{oc} \sim 0.44$V, FF ~ 0.55 and $\eta \sim 2.7\%$.

Data are now available for the cells from the first group which were examined at IEC. Screen printing was used to define a 1 cm^2 cell area in the center of the substrate. The heterojunctions were then surveyed by a laser scan method to varify photovoltaic response and check the uniformity. The results of this evaluation are given in Table I. Five of the substrates were selected for fabrication into cells using the standard IEC procedures. The Au grid electrode consisted of 0.012 mm wide lines with 0.32 mm line-to-line spacing. After initial testing the cells were optimized by heat treatment. Heat treatments at 170°C in a H_2 ambient and at 130°C, 150°C and 170°C in vacuum were employed. The maximum performances achieved during the heat treatments are summarized in Table II. The cells all yielded efficiencies of about 2% or better. The highest efficiency was 5.74% (no AR coating) for cell 1604.

TABLE I

LASER SCAN EVALUATION OF Cu_2S UNIFORMITY
(Sputtered Cu_2S/Evaporated CdS Hybrid Cells)

Telic Cell Number	IEC Substrate	Cu_2S Thickness	Cu_2S Temperature	Uniformity observation (As-deposited state)
1607	1016	75 nm	$\sim 40^{\circ}C$	non-uniform, fingerprints
1613	1047	75 nm	$\sim 120^{\circ}C$	non-uniform, discontinuous
1589	1016	150 nm	$\sim 40^{\circ}C$	uniform, weak response
1604	1016	150 nm	$\sim 140^{\circ}C$	uniform, strong response
1601	1016	300 nm	$\sim 40^{\circ}C$	non-uniform, weak response
1610	1047	300 nm	$\sim 120^{\circ}C$	very large dead zone

TABLE II

MAXIMUM PERFORMANCE OF HYBRID CELLS EXAMINED AT IEC
(Sputtered Cu_2S/Evaporated CdS)

Telic cell number	IEC substrate number	Cu_2S thickness	Cu_2S temp.	Cu_2S resistivity	Anneal[3] time	J_{sc}[4]	V_{oc}	FF	η[5]
1607	1016 (1)	75 nm	~40°C	$1.2\times10^{-2}\ \Omega$-cm	Not tested - non uniform Cu_2S layer.			(see Table I)	
1613	1047 (2)	75 nm	~120°C	$3.4\times10^{-2}\ \Omega$-cm	96 hr	10.55 mA/cm^2	0.46V	0.52	2.68%
1589	1016 (1)	150 nm	~40°C	$3.7\times10^{-3}\ \Omega$-cm	192 hr	9.82 mA/cm^2	0.49V	0.66	3.67%
1604	1016 (1)	150 nm	~140°C	$2.9\times10^{-2}\ \Omega$-cm	64 hr	17.89 mA/cm^2	0.47V	0.60	5.74%
1601	1016 (1)	300 nm	~40°C	$5.0\times10^{-3}\ \Omega$-cm	192 hr	5.95 mA/cm^2	0.43V	0.55	1.60%
1610	1047 (2)	300 nm	~120°C	$6.7\times10^{-2}\ \Omega$-cm	47 hr	13.26 mA/cm^2	0.44V	0.55	3.69%

(1) CdS thickness = 27 μm, resistivity = 1.4 Ω-cm.

(2) CdS thickness = 33 μm, resistivity = 2.4 Ω-cm.

(3) Heat treatments were made at 170°C in 100%-H_2 to increase the short circuit current. Typical durations were 16 or 64 hrs. These treatments were alternated with vacuum heat treatments at 130°C for 16 hrs to increase the open circuit voltage.

(4) Tested under simulated solar illumination at 87.5 mW/cm^2.

(5) No antireflection layer.

In general, the lowest efficiencies in Table II were obtained with cells having nonuniform laser scan responses. The cells listed in the table were the first group that was fabricated in the Cu_2S hybrid series. Significant improvements in uniformity and efficiency can be expected when Telic has accumulated more experience in the handling of the IEC substrates and particularly in performing the pre-deposition HCl etch step. It should also be noted that the cells shown in Table II were tested at a light intensity of 87.5 mW/cm^2. Thus at 100 mW/cm^2 the J_{sc} of cell 1604 (17.89 mA/cm^2) would correspond to 20.45 mA/cm^2. With an AR coating, this would be expected to reach about 22 mA/cm^2, which is in the range achieved by conventional wet processing in the high performance IEC cells.

It is difficult to relate the performance of the Delaware cells to the specific Cu_2S sputter deposition conditions because of the spatial nonuniformity in some of the Cu_2S layers. The best performance was achieved with a cell (1604) having a 150 nm thick Cu_2S layer which was deposited at 120°C and exhibited an as-deposited resistivity of about $3x10^{-2}\Omega$-cm. The I-V characteristic for this cell is shown in Fig. 7 and compared to a cell (1589) with a Cu_2S layer of similar thickness, but which was deposited at 40°C and had a lower as-deposited resistivity of about $4x10^{-3}\Omega$-cm. Figure 8 shows the I-V characteristics for two cells (1610 and 1613) which were deposited at 120°C and have as-deposited resistivities that are comparable to the high performance cell ($4\text{-}7x10^{-2}\Omega$-cm) but thicknesses that are above (300 nm) or below (75 nm) the value (150 nm) for the best cell.

The superior performance of the cells heat treated at IEC in pure H_2 at 170°C, as compared to those processed at Lockheed in Ar-2% H_2 at 155°C, suggests that the pure H_2 may permit advantages not obtainable with more diluted mixtures. Therefore provisions to use pure H_2 are being incorporated into the Lockheed annealing apparatus.

The best performances in the Lockheed studies were also achieved with cells having Cu_2S layers with the higher as-deposited resistivities ($\sim 10^{-2}\Omega$-cm). The dependence of J_{sc} on the Cu_2S thickness and resistivity in these cells

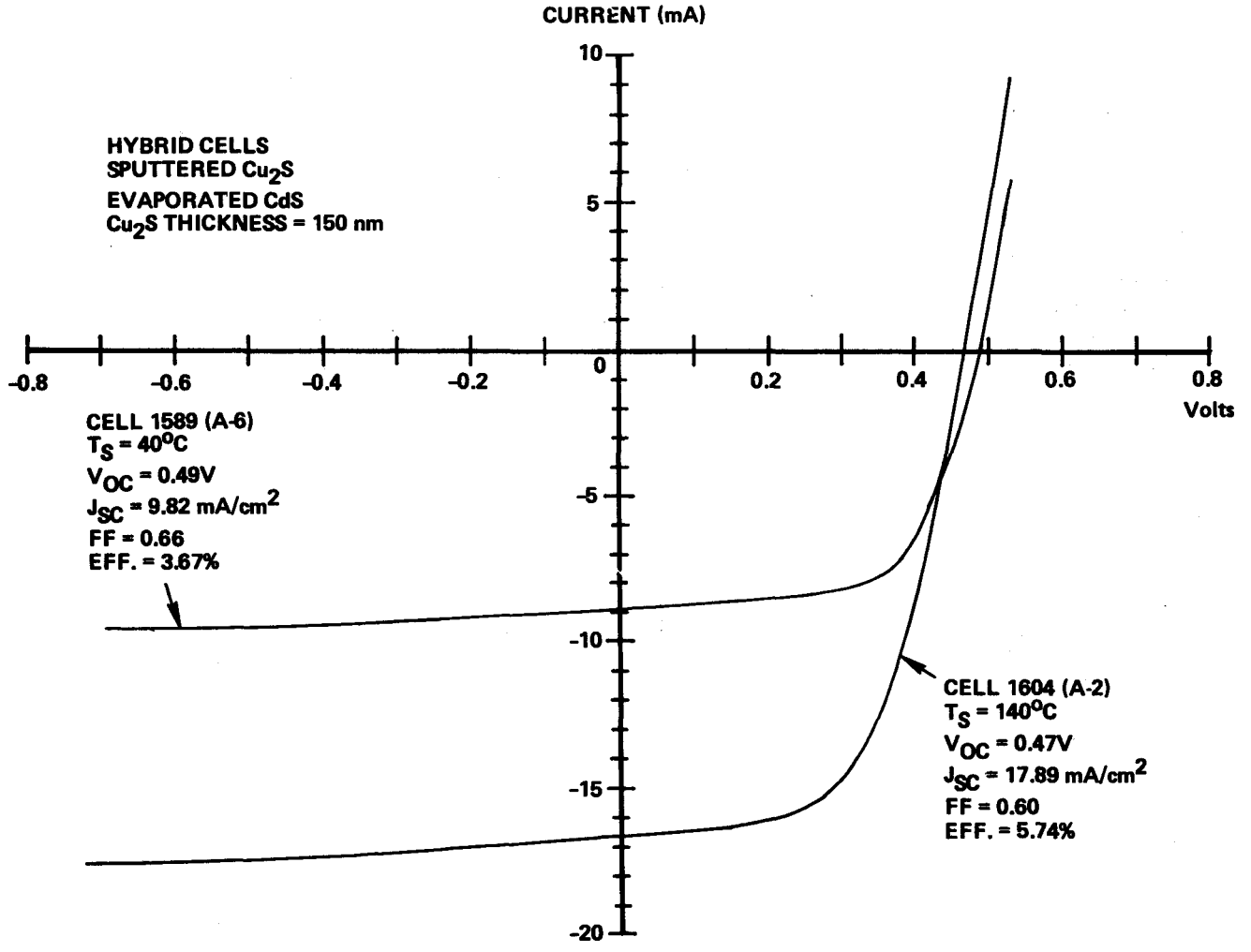

FIG. 7 I-V characteristics for hybrid (sputtered-Cu_2S/evaporated CdS) cells having Cu_2S layers deposited at different substrate temperatures.

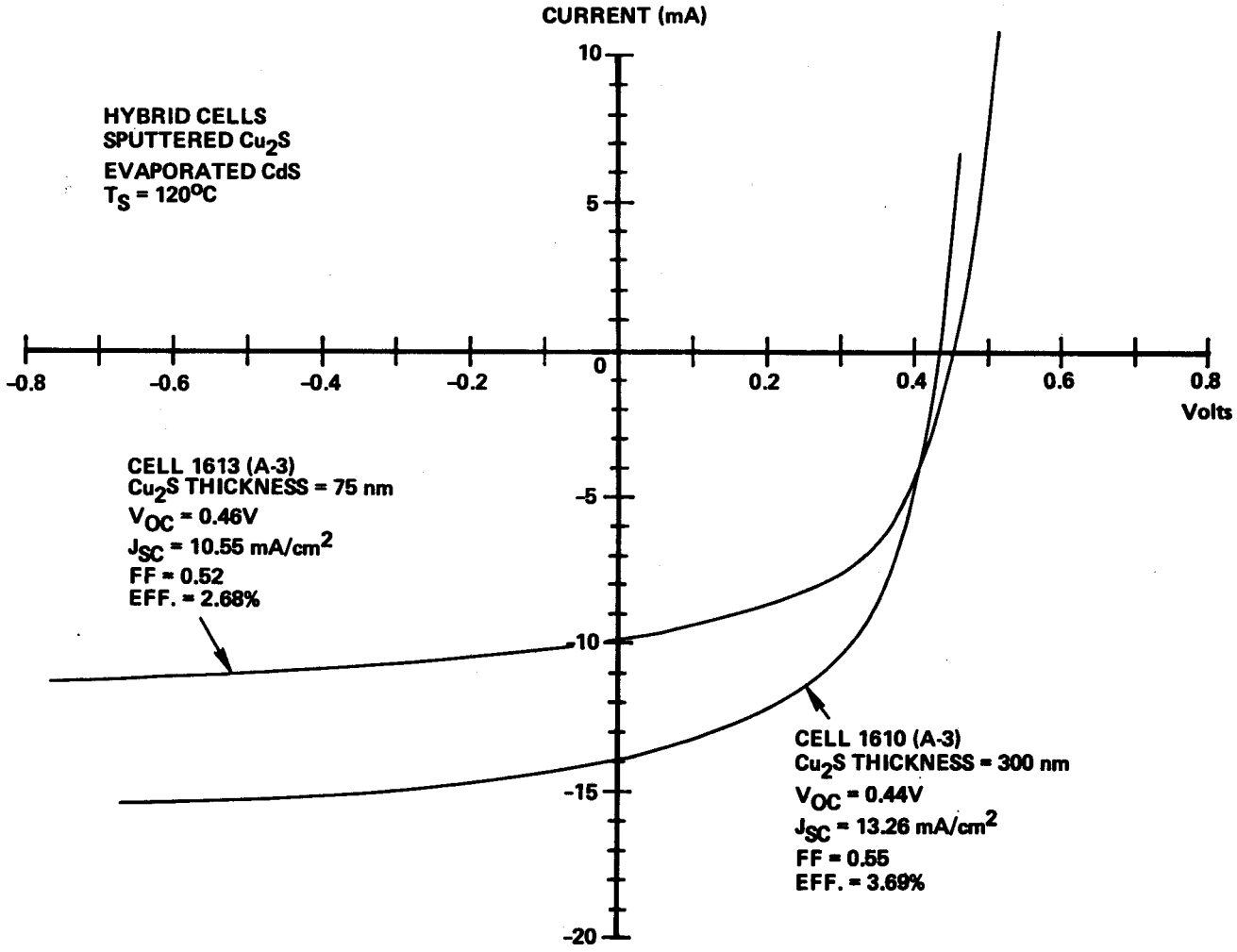

FIG. 8 I-V characteristics for hybrid (sputtered-Cu_2S/evaporated CdS) cells having Cu_2S layers of different thicknesses.

suggested that the performance of the Cu_2S layer may have been limited by a low minority carrier diffusion length. Therefore a second series of cells was fabricated under conditions (shaded area on curve b in Fig. 6) which yielded higher resistivities ($\sim$0.5 Ω-cm) and probably more stoichiometric as-deposited coatings. The deposition procedures were identical to those described in Ref. 1 for the first series of cells. The specific deposition conditions are listed below.

Discharge current = 1 Ampere.
Discharge current density = 4.7 mA/cm^2.
Discharge voltage = 1260V.
H_2S injection rate = 4.5×10^{18} molecules/sec (17 Pa-liters/sec).
Deposition rate = 0.75 nm/s.
Substrate temperature $\sim$40°C.
Coating thicknesses = 75 nm, 150 nm and 300 nm.
Cathode conditioning = 5 min at the deposition conditions.

Two heterojunctions were fabricated in each deposition run. One heterojunction from each run was sent to IEC. The other was given a Au top grid electrode and sent to Lockheed. Data are available on the results of Lockheed heat treatment studies using Ar-2% H_2 at 155°C. These results are summarized in Table III. The more stoichiometric Cu_2S may have increased the current which can be collected from the thicker Cu_2S layers; however, the V_{oc} and FF values are low.

Figure 9 shows the spectral response of the short circuit current under 28% of AM1 illumination for the three cells shown in Table III. The response, particularly at the shorter wavelengths, is significantly decreased in the cell with the thick (300 nm) Cu_2S layer. Significant absorption in the CdS is seen for the cell with the thin (75 nm) Cu_2S layer.

4. IMPROVED DEVICE DESIGN

Progress has been made in improving the mask hold-down and therefore the definition of the Au-grid top electrodes that are applied at Telic.

In the cells fabricated thusfar the top grid electrodes have been applied by sputtering using a cylindrical magnetron source. This source is capable of

TABLE III

MAXIMUM PERFORMANCE OF SECOND SERIES OF HYBRID CELLS PROCESSED AT LOCKHEED

(Sputtered Cu_2S/Evaporated CdS)

Telic cell number	IEC substrate number	Cu_2S thickness	Cu_2S temp.	Cu_2S resistivity	Anneal[3] temp.	Anneal time	J_{sc}[4]	V_{oc}	FF	η
1780	2-1055 (1)	300 nm	~40°C	0.54 Ω-cm	~155°C	~18 hrs	5.66 mA/cm^2	0.33V	-	-
1783	2-1055 (1)	150 nm	~40°C	0.42 Ω-cm	~155°C	~18 hrs	11.78 mA/cm^2	0.37V	0.49	1.9%
1786	2-1055 (1)	75 nm	~40°C	0.45 Ω-cm (2)	~155°C	~18 hrs	10.49 mA/cm^2	0.38V	0.38	1.5%

(1) CdS thickness = 31 μm, resistivity = 2.9 Ω-cm.

(2) Estimated value.
In-situ resistivity sample not available.

(3) Anneal atmosphere, Ar-2% H_2.

(4) Tested under simulated solar illumination at 100 W/cm^2.

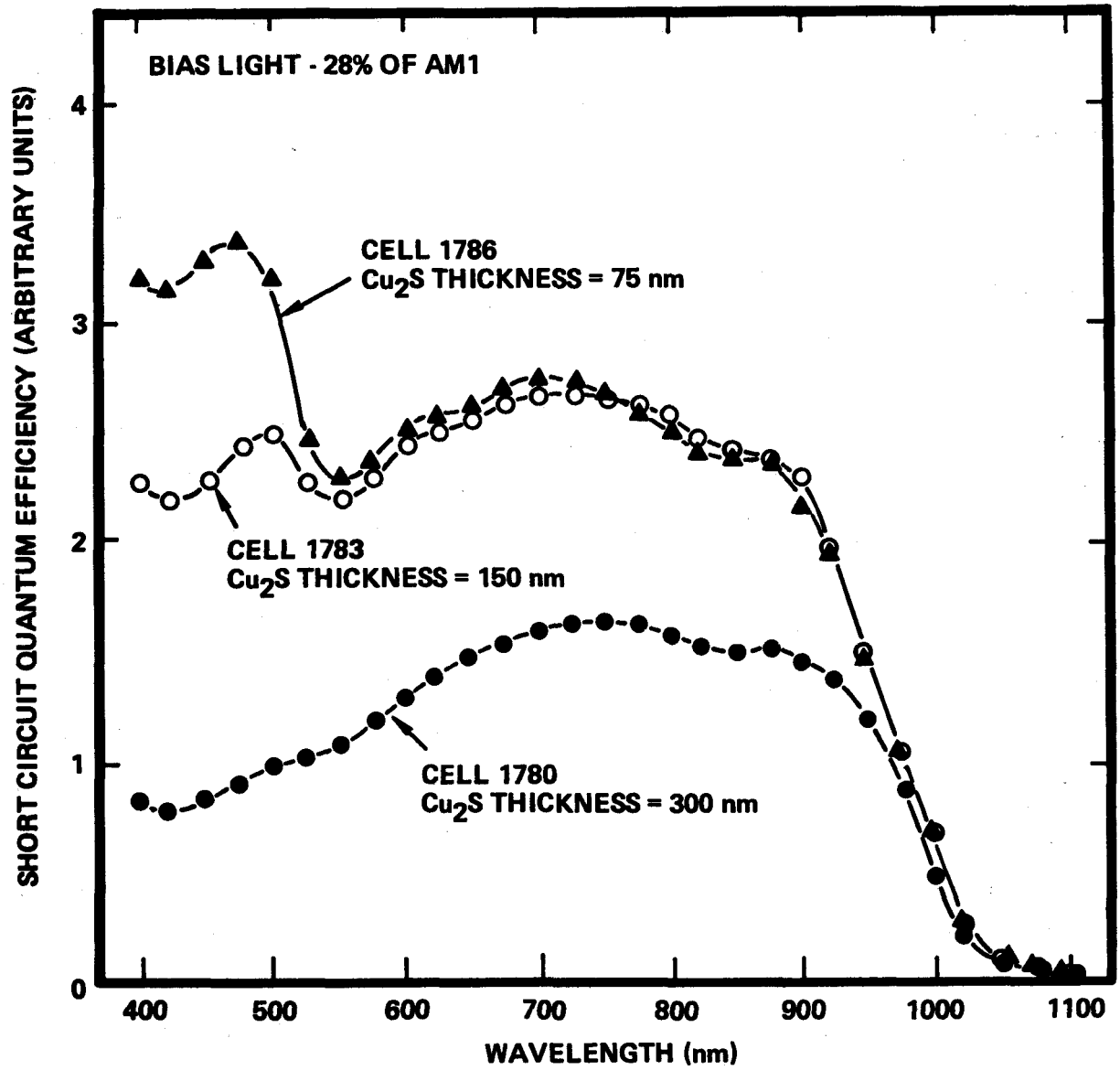

FIG. 9 Relative spectral response of short circuit current in hybrid (sputtered Cu_2S/evaporated CdS) cells having Cu_2S layers of different thicknesses. (See Table III.)

depositing grid electrodes on a large number of substrates at one time, but makes inefficient use of the gold when only a few substrates are to be coated. Typically three cells are fabricated during a given CdS/Cu_2S deposition run in the multi-source chamber. Therefore a simple resistively-heated evaporated system has been designed and is being installed in the grid deposition chamber. The evaporation system will permit efficient use of gold while adding grids to as few as three up to as many as nine substrates.

5. PLANAR MAGNETRON SPUTTERING

A 5 inch x 12 inch planar magnetron with a 99.9999% Cd target has been mounted at one of the source positions in the deposition chamber shown in Fig. 4. The potential advantage of the planar magnetron is that the nonuniform current density may permit some regions of the cathode surface to remain unpoisoned[8] by H_2S reactions under conditions where CdS coatings are formed at the substrate. The high Cd flux from the unpoisoned regions may then permit nonstoichiometric coatings with a greater excess of Cd and a lower resistivity to be deposited than were possible with the cylindrical magnetron sources.

Figure 10 shows the CdS deposition rate versus the H_2S injection rate for the planar magnetron, compared to similar data for a cylindrical magnetron.[2,9] The deposition rates were determined from interferometric measurements of the thicknesses of coatings about 100 nm thick, by using a Sloan Angstrometer--Tolansky method.[10] Both sources were operated at the same total discharge current, with the substrates maintained at 250°C.

The H_2S injection rates were controlled and measured with a Tylan mass flow controller. The scale at the top of the figure refers to the H_2S partial pressure measured with a capacitive manometer prior to igniting the plasma discharge. The nonlinear relationship between the H_2S partial pressure and the H_2S injection rate, at injection rates greater than about 70 Pa-liters/sec, is a consequence of exceeding the capacity of the oil diffusion pump. When the discharge is ignited much of the injected H_2S is consumed by the reactive sputtering process. Although H_2 is liberated, the measured pressure varied linearly with the H_2S

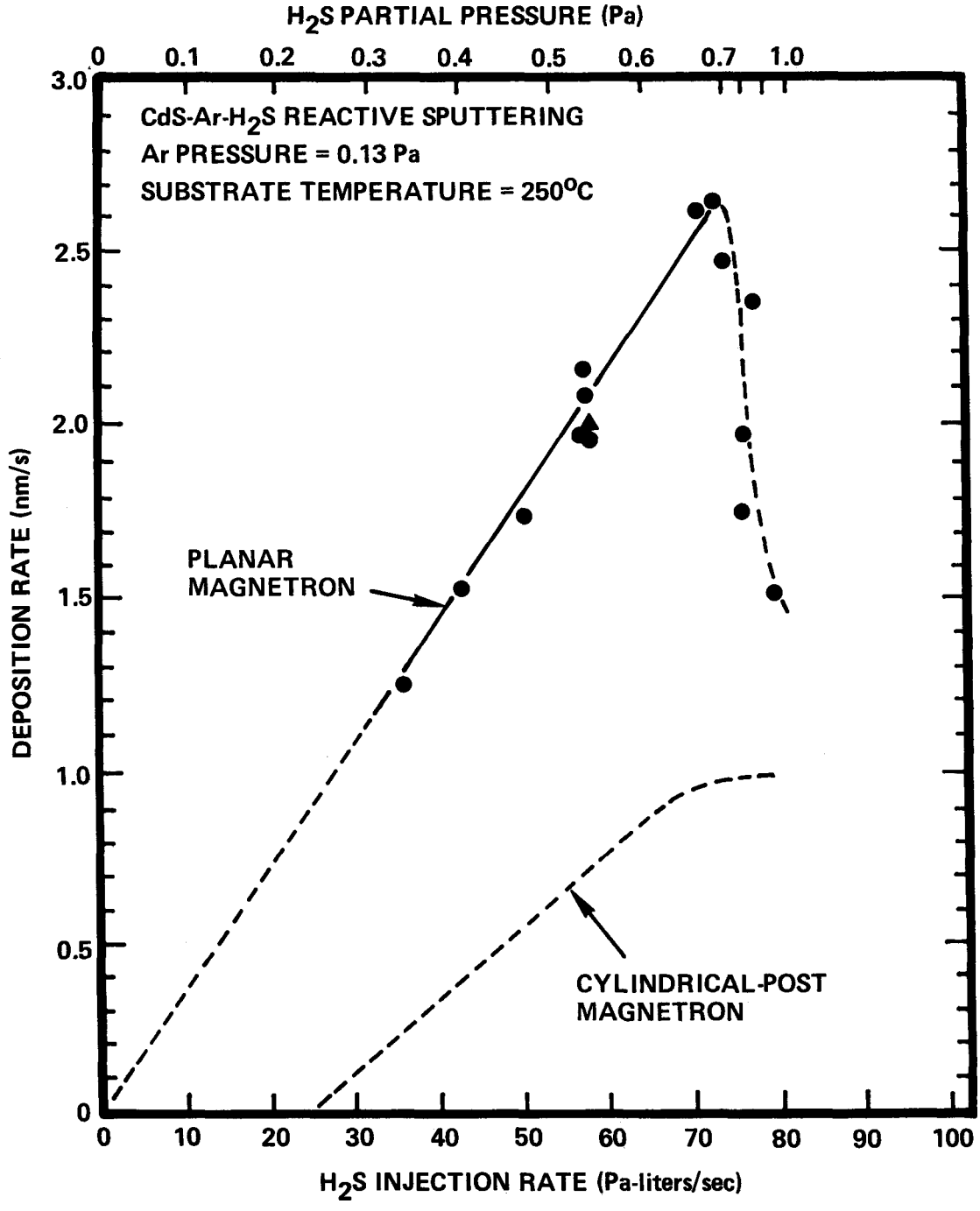

FIG. 10 Deposition rate versus H_2S injection rate for reactive sputtering of CdS using planar magnetron sputtering source. Cylindrical-post magnetron data from refs. 2 and 9 shown for comparison. Discharge current for both sources 1A. Upper scale shows H_2S partial pressure prior to igniting discharge.

injection rate over the range examined. This linear variation indicates that the pump capacity was not exceeded during the actual deposition process.

It should be noted that the reactive gas injection rate is often a more fundamental parameter in the chemistry of reactive sputtering than the partial pressure. This is seen to be the case here, at least insofar as the deposition rate is concerned. Thus the triangular planar magnetron data point in Fig. 10 at an injection rate of 57 Pa-liters/sec was obtained with a reduced gate valve opening (effective pumping speed) which yielded an initial partial pressure of about 1 Pa. The resulting deposition rate is seen to be consistent with that obtained at an identical injection rate but higher pumping speed.

The linear range of the planar and cylindrical magnetron deposition rate data in Fig. 10 is believed to result from operating under conditions where the sulfur flux is rate limiting. The decrease in deposition rate for the cylindrical magnetrons at high H_2S injection rates has been interpreted as a condition where the deposition rate is limited by the available sputtered Cd flux.[2,9] Note that the planar magnetron data differ from the cylindrical data in two ways: (1) the linear region projects through zero in the planar case, while a critical H_2S injection rate was required to achieve deposition in the cylindrical case; and (2) the planar magnetron deposition rates decreased abruptly at high H_2S injection rates. The requirement of a critical H_2S injection rate to achieve deposition in the cylindrical magnetron case may be the consequence of cathode poisoning. Sputtering at poisoned cathodes is known to produce active species which are passed to the substrates. These species could be the precursors which allow deposition on the hot substrate to begin. The non-linear current density in the planar magnetron case causes some regions of the cathode surface to be poisoned even at very low reactive gas injection rates.

The sputtered flux from a cylindrical magnetron passes radially outward in all directions while the flux from a planar magnetron passes more nearly in one direction. Thus simple geometric considerations dictate that the local deposition rate from a planar magnetron be about three times larger than that

at an equivalent distance from a cylindrical source of identical length operating under identical conditions. In the present experiments the effective lengths of the two sources were comparable. The source-to-substrate distance was 7.6 cm for the planar magnetron, compared to 8.9 cm for the cylindrical case. Referring to Fig. 10, one sees that the planar magnetron deposition rate is about three times larger than the cylindrical magnetron rate for the range of H_2S injection rates that yielded the highest deposition rates. Thus sputtering from non-poisoned regions of the planar cathode did not yield disportionately high deposition rates.

Figure 11 shows the CdS reactive sputtering deposition rate versus substrate temperature for the planar magnetron, again compared to similar data from cylindrical magnetrons.[9] Both sources were operated at the same total discharge current and H_2S injection rate. The planar magnetron data imply an activation energy of about 0.26 eV. This is compared to an activation energy of about 0.45 eV for the cylindrical magnetrons. An activation energy of $\sim$0.40 eV was reported for epitaxial deposition in a quasi-closed cell and attributed to desorption of the Cd and S atoms.[11]

Figure 12 shows the CdS resistivity as a function of H_2S injection rate for the planar and cylindrical magnetrons operated at a substrate temperature of 250°C and a common discharge current. The resistivities were measured using a pattern of Nb electrodes which was deposited onto the CdS in the multi-source chamber without breaking vacuum. The data imply that an abrupt decrease in resistivity occurs as the H_2S injection rate is decreased to a value corresponding approximately to passage onto the linear portions of the curves shown in Fig. 10. Similar abrupt decreases in resistivity were observed in In doping studies and attributed to a reduction in the Cd vacancy level when deposition was carried out under conditions which were deficient in sulfur (H_2S flux was rate limiting).[9] Under these conditions the planar magnetron resistivities are indeed lower than those produced by the cylindrical magnetrons, and are about equal to those previously obtained at a substrate temperature of 250°C with the pulsed gas injection method,[2] or when a previously deposited CdS

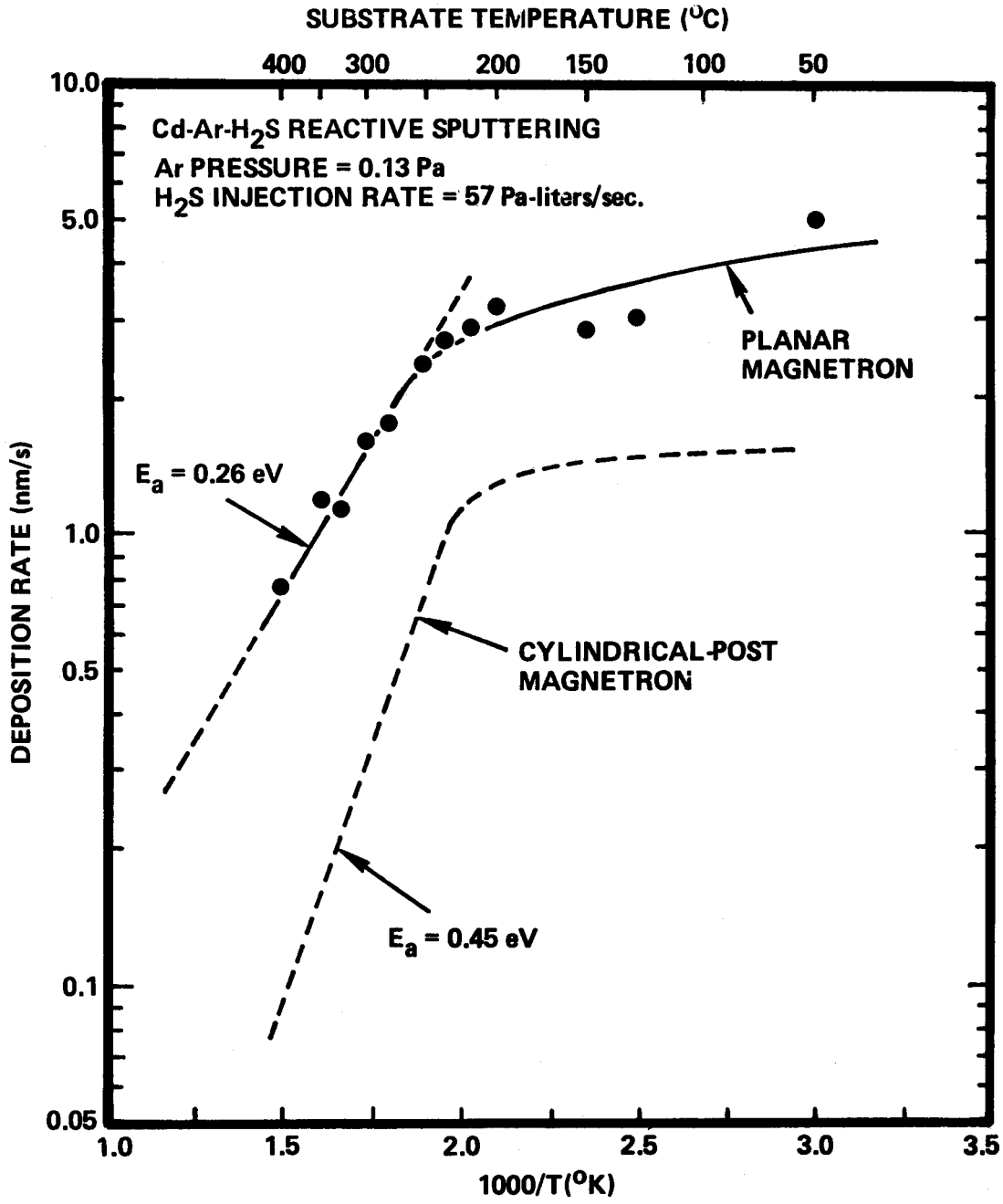

FIG. 11 Deposition rate versus substrate temperature for reactive sputtering of CdS using planar magnetron sputtering source. Cylindrical-post magnetron data from ref. 9 shown for comparison. Discharge current for both sources 1A.

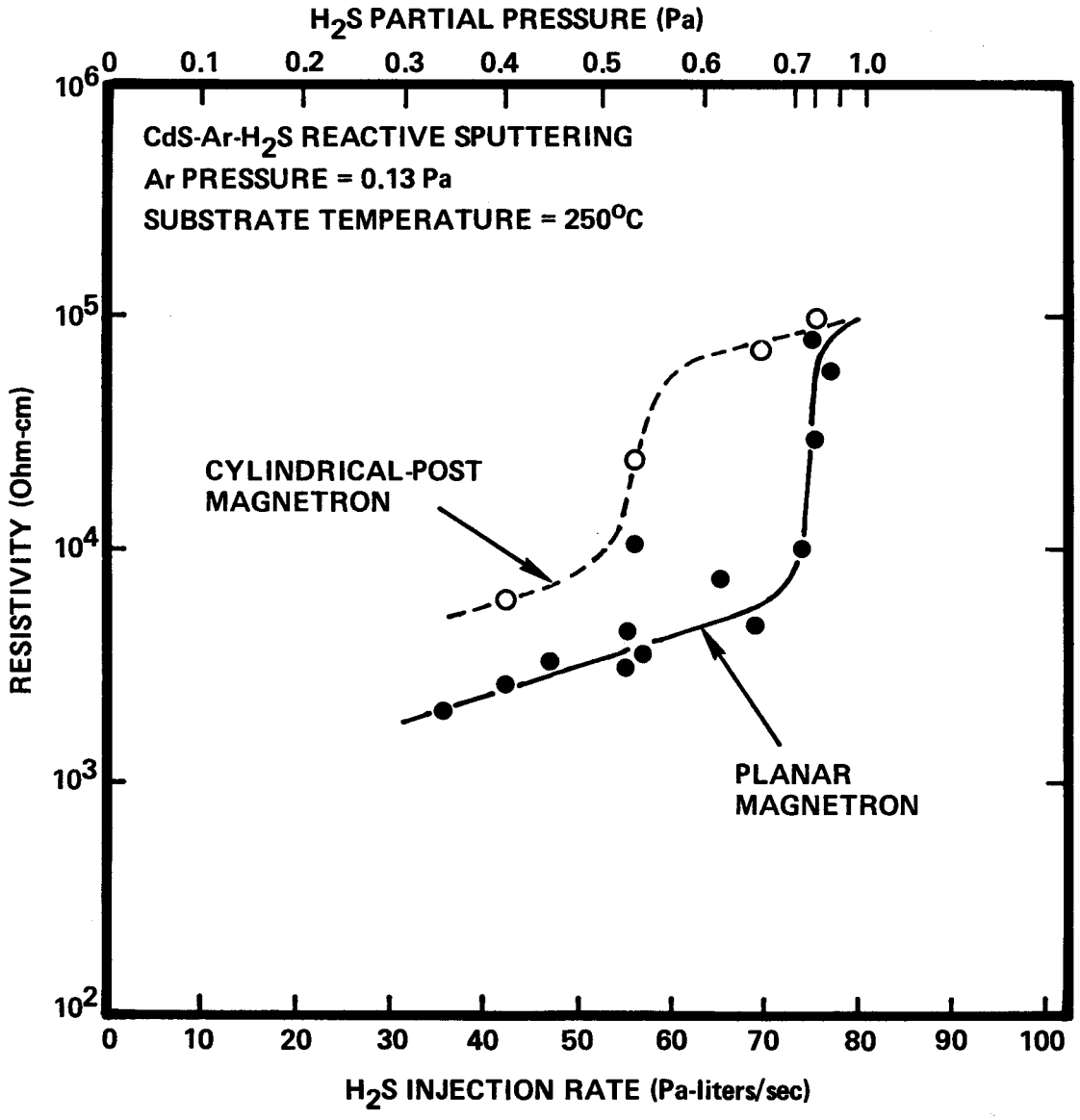

FIG. 12 Resistivity versus H_2S injection rate for reactive sputtering of CdS using planar magnetron sputtering source. Cylindrical-post magnetron data from ref. 2 shown for comparison. Discharge current for both sources 1A. Upper scale shows H_2S partial pressure prior to igniting discharge.

coating was given a post-deposition heat treatment by maintaining it for about 5 min at 250°C in a sputtered Cd flux.[2]

Figure 13 shows the CdS resistivity as a function of substrate temperature for the planar magnetron, compared to cylindrical magnetron data that were reported previously. Both sources were operated at the same total discharge current and H_2S injection rate. The H_2S injection rate was within the linear (H_2S-rate-limited) region for both sources. The planar magnetron resistivities are seen to be comparable to or less than those obtained with the cylindrical magnetron.

Visual photoluminescence at liquid nitrogen temperatures has been observed for 3000 nm thick CdS coatings deposited onto Nb coated glass, at 250°C with H_2S injection rates of 57 and 70 Pa-liters/sec, using the planar magnetron. Coatings of this thickness, deposited under similar conditions with the cylindrical magnetrons, did not exhibit visible photoluminescence (see Section 2.2).

Future work will involve cell fabrication using the CdS deposited by the planar magnetron.

6. DEVICE CHARACTERIZATION AND FABRICATION

Work at Lockheed during this reporting period has involved characterization and heat treatment studies on all-sputter-deposited (Section 2.3) and hybrid cells with sputtered Cu_2S layers (Section 3.2). Improvements are being made to the heat treatment oven to permit the use of pure H_2, since the IEC work indicates that pure H_2 is more effective than diluted H_2-Ar mixtures. Improvements are also being made in the methods of performing C-V measurements and analysis, in anticipation of probing the junctions in all-sputtered cells. In the course of this work a frequency dispersion analysis has been developed which permits a determination of the surface resistance of the Cu_2S layer. The surface resistivity predicted by this method, from C-V measurements made on one of the hybrid cells listed in Table III, was in excellent agreement with the value measured at Telic on the Cu_2S coating that was deposited onto a glass substrate during the heterojunction fabrication. The frequency dispersion analysis is described in Appendix A.

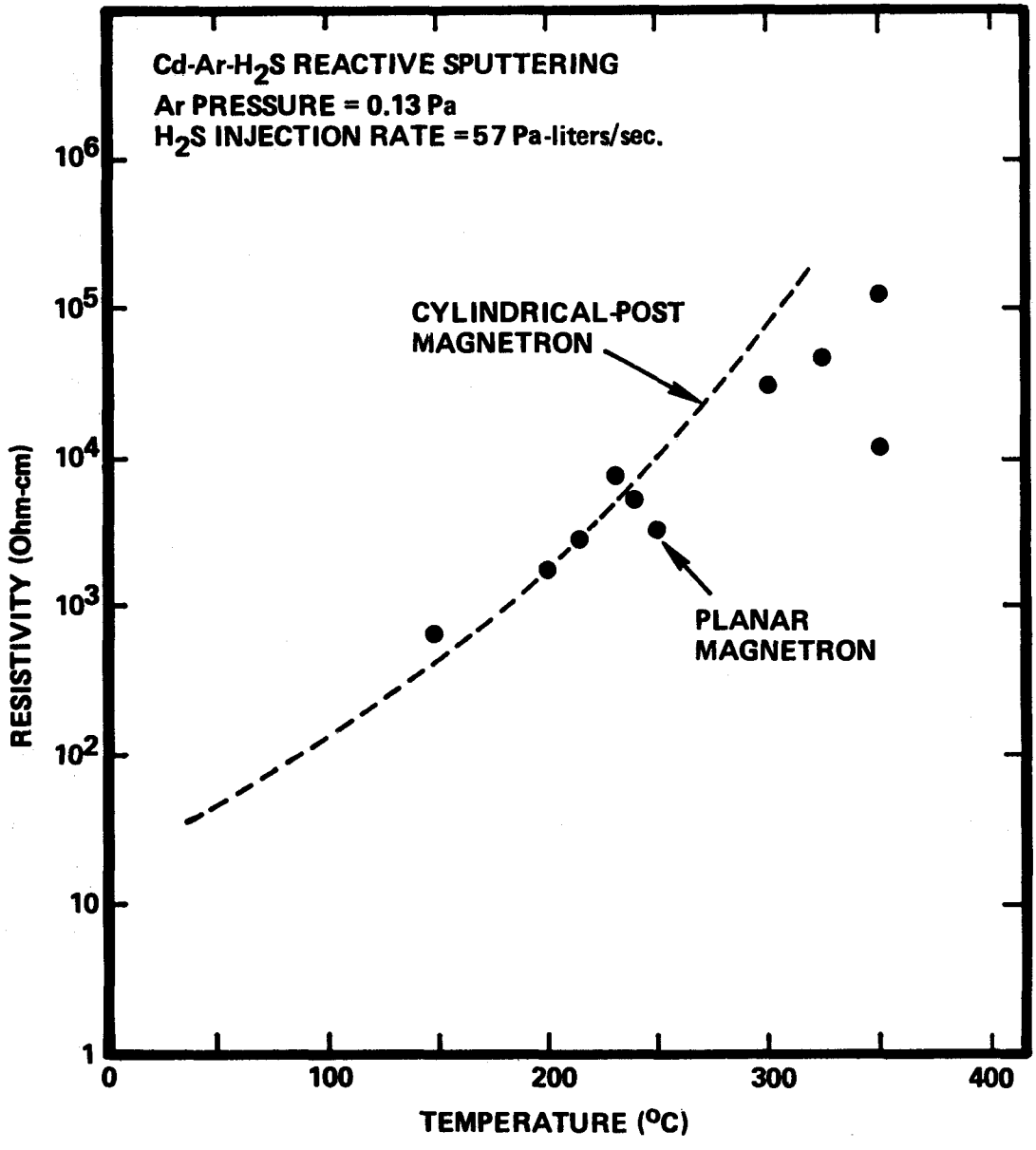

FIG. 13 Resistivity versus substrate temperature for reactive sputtering of CdS using planar magnetron sputtering source. Cylindrical-post magnetron data from ref. 2 shown for comparison. Discharge current for both sources 1A.

Work at IEC has involved photoluminescence measurements on sputter-deposited CdS (Section 2.2) and characteriztion and heat treatment studies on hybrid cells with sputtered Cu_2S layers (Section 3.2). Additional Cu_2S hybrid cells have been sent to IEC and are under evaluation. Procedures are being developed to form hybrid cells with sputtered CdS layers as a means of evaluating the sputtered CdS. Sputtered CdS coatings on Nb coated glass have been sent to IEC to assist in this task.

7. SUMMARY STATUS

Significant progress has been made on all of the research tasks.

Photoluminescence spectral measurements on 6000 nm thick cylindrical magnetron reactive sputtered CdS coatings have yielded exciton and "green edge emission" spectra which are similar in their general character to that of the evaporated CdS that yields high performance cells. Visual photoluminescence emission has been observed from 3000 nm thick CdS coatings prepared by planar magnetron reactive sputtering. Samples have been sent to IEC for photoluminescence spectral measurements. Future work will attempt to correlate the photoluminescence spectra with the performance of the sputtered CdS when used in cells. This work should provide an improved understanding of the significance of the photoluminescence spectra in terms of cell performance, for CdS prepared by both evaporation and sputtering methods.

Planar magnetron CdS reactive sputtering experiments have begun. Data has been obtained on the dependence of the deposition rate and coating resistivity on the substrate temperature and H_2S injection rate. The planar magnetron data are generally consistent with data previously reported for CdS reactive sputtering using cylindrical-post magnetrons. The directed flux from the planar magnetron yields a deposition rate at the substrate position that is about a factor of three larger than that for the cylindrical magnetrons under equivalent operating conditions. The coating resistivities obtained with the planar magnetron under typical operating conditions are several times lower than those obtained with the cylindrical magnetrons. This may be a consequence of the

concentrated cathode current densities which could increase the Cd/S ratio of the emission flux from the planar magnetron source.

Cu_2S reactive sputtering experiments have further elucidated the influence of the cathode and wall conditioning on the deposition process. A hybrid cell with sputtered Cu_2S deposited onto evaporated CdS supplied by IEC and heat treated in pure H_2 at IEC has yielded $J_{sc} \sim 18$ mA/cm^2 (under illumination of 87.5 mW/cm^2), V_{oc} = 0.47V, FF = 0.60 and η = 5.74% with no AR coating. Several other cells yielded efficiencies of about 3% or greater. These results were obtained in the first attempt to form hybrid cells with sputtered Cu_2S layers. Thus, although the sputtered Cu_2S in these devices was somewhat nonuniform and probably not optimum, the results confirm that sputtered Cu_2S layers of sufficient quality to evaluate the sputtered CdS can be deposited. They also show that sputtering may provide an effective Cu_2S deposition method that could be used in combination with evaporation to provide an all vacuum cell production method. Several of the hybrid cells have provided current densities which exceed the second quarter goal of $J_{sc} \sim 10$ mA/cm^2. However, high current densities have yet to be achieved with the all-sputter-deposited cells.

All-sputter-deposited cells which incorporate composite CdS layers consisting of In-doped and undoped regions have yielded $J_{sc} \sim 3$ mA/cm^2, $V_{oc} \sim 0.44$V, and FF ~ 0.3. Although this performance is poor, it exceeds that previously obtained[2] for this structure, which is designed to increase the junction electric field and is one of the important approaches planned for investigation on the present program.

An analysis has been made at Lockheed which relates a frequency dispersion which is observed in C-V measurements on CdS/Cu_2S solar cells to the surface resistivity of the Cu_2S layer.

Work during the third quarter will involve additional studies to elucidate the Cu_2S reactive sputtering mechanism. Additional hybrid cells with sputtered Cu_2S on evaporated CdS will be deposited to repeat and confirm the high-performance achieved in the cells fabricated thusfar. Hybrid cells with (CdZn)S evaporated layers will be fabricated as soon as evaporated (CdZn)S substrates

are available from IEC. A systematic study will be made of the CdS layers deposited by the planar magnetron reactive sputtering method and their performance in cells. Each deposition run will fabricate two all-sputtered cells and one reference CdS coating for resistivity measurements (through the film) and photoluminescence and scanning electron microscopy observations. The variables will be the substrate temperature and the H_2S injection rate. Post-deposition heat treatment will also be examined. Finally it is planned that all-sputtered cells with composite "CdS" layers, consisting of In-doped CdS adjacent to the rear electrode and (CdZn)S adjacent to the junction, will be fabricated using the cylindrical-post magnetron sources.

REFERENCES

1) J. A. Thornton, W. W. Anderson and J. D. Meakin, "Cadmium Sulfide/Copper Sulfide Heterojunction Cell Research by Sputter Deposition," Qtr. Rept. Sept. 2, 1980 to Nov. 30, 1980, SERI Contract XW-Ø-9296, Telic Corporation Santa Monica, CA (Dec. 1980).

2) J. A. Thornton and D. G. Cornog, "Cadmium Sulfide/Copper Sulfide Heterojunction Cell Research," Final Report, Feb. 26, 1979 to July 15, 1980, SERI Contract XJ-9-8033-2, Telic Corporation, Santa Monica, CA (June 1980).

3) R. E. Halsted, "Edge Emission," in Physics and Chemistry of II-VI Compounds, ed. M. Aven and J. S. Prener, North-Holland, New York (1967) pp. 385-431.

4) M. H. Christman, K. A. Jones and K. H. Olsen, "Formation of Hexagonal Pyramids and Hexagonal Flat Tops on the Surface of Heteroepitaxial (0001) CdS Films," J. Appl. Phys. 45, 4295 (1974).

5) R. B. Hall, R. W. Birkmire, E. Eser, T. L. Hench and J. D. Meakin, "Growth and Evaluation of CdS and (CdZn)S Films for the Fabrication of High Performance Photovoltaic Devices," Proceedings 14th IEEE Photovoltaic Specialists Conf., San Diego, CA (Jan. 1980) p. 706.

6) J. A. Thornton, "Cadmium Sulfide/Copper Sulfide Heterojunction Research," Qtr. Rept., June 1, 1979 to Sept. 30, 1979, SERI Contract XJ-9-8033-2, DOE Report DSE-4042-T19 (Nov. 1979). Available from National Technical Information Service, U.S. Dept. of Commerce, Springfield, VA 22161.

7) A. D. Jonath, W. W. Anderson, J. A. Thornton and D. G. Cornog, "Copper Sulfide Films Deposited by Cylindrical Magnetron Reactive Sputtering," J. Vac. Sci. Technol. 16, 200 (1979).

8) S. Schiller, U. Heisig and K. Goedicke, "Advances in High Rate Sputtering with Magnetron-Plasmatron Processing and Instrumentation," Thin Solid Films, 64, 455 (1979).

9) J. A. Thornton, D. G. Cornog and W. W. Anderson, "Indium Doped Cadmium Sulfide Films Deposited by Cylindrical Magnetron Reactive Sputtering," J. Vac. Sci. Technol. 18 (1981).

10) W. A. Pliskan and S. J. Zanin, "Film Thickness Composition," in Handbook of Thin Film Technology, ed. L. I. Maissel and R. Glang, McGraw-Hill, New York (1970) p. 11-1.

11) I. P. Kalinkin, N. S. Bogomolov, V. A. Sanitarov and L. N. Aleksandov, "The Regularities of Growth and Properties of Epitaxial Cadmium Chalcogenide Films Condensed from a Gas Phase of Controlled Composition," Thin Solid Films 66, 25 (1980).

APPENDIX A

Analysis of Dispersion in Measured Capacitance of CdS/Cu_2S Solar Cells

W. W. Anderson
Lockheed Palo Alto Research Laboratory

Dispersion in the measured capacitance of CdS/Cu_2S cells was noted during an attempt to apply C-V techniques to an analysis of junction space charge density under illumination. As a consequence the significance of $1/c^2$ vs V plots obtained at different frequencies was questionable. A simple analysis indicated that the problem is associated with the distribution of current flow in the Cu_2S layer to the contact finger grids.

Figure 1 is a schematic sketch of a portion of a Cu_2S/CdS cell. Assume that the Au contact grids and the bulk CdS form two equipotential regions. The Cu_2S layer then forms a distributed series resistance and the CdS depletion layer forms a distributed shunt capacitance. If the cell consists of n identical periods, then the cell conductance may be obtained from 2n of the elementary lossy transmission lines shown in Figure 2. The open circuit boundry condition at x = s results from symmetry considerations wherin there is no lateral current flow midway between Au current collection fingers. The capacitance per unit length of line is given by:

$$c = C_o L$$

and the resistance per unit length by:

$$r = R_\square / L$$

where C_o is the depletion layer capacity per unit area and $R_\square$ is the Cu_2S sheet resistance per square ($R_\square = \rho / t$). For sinusoidal excitation, the differential equations for current and voltage along the line are:

$$\frac{di}{dx} = -j\omega c v \qquad (1)$$

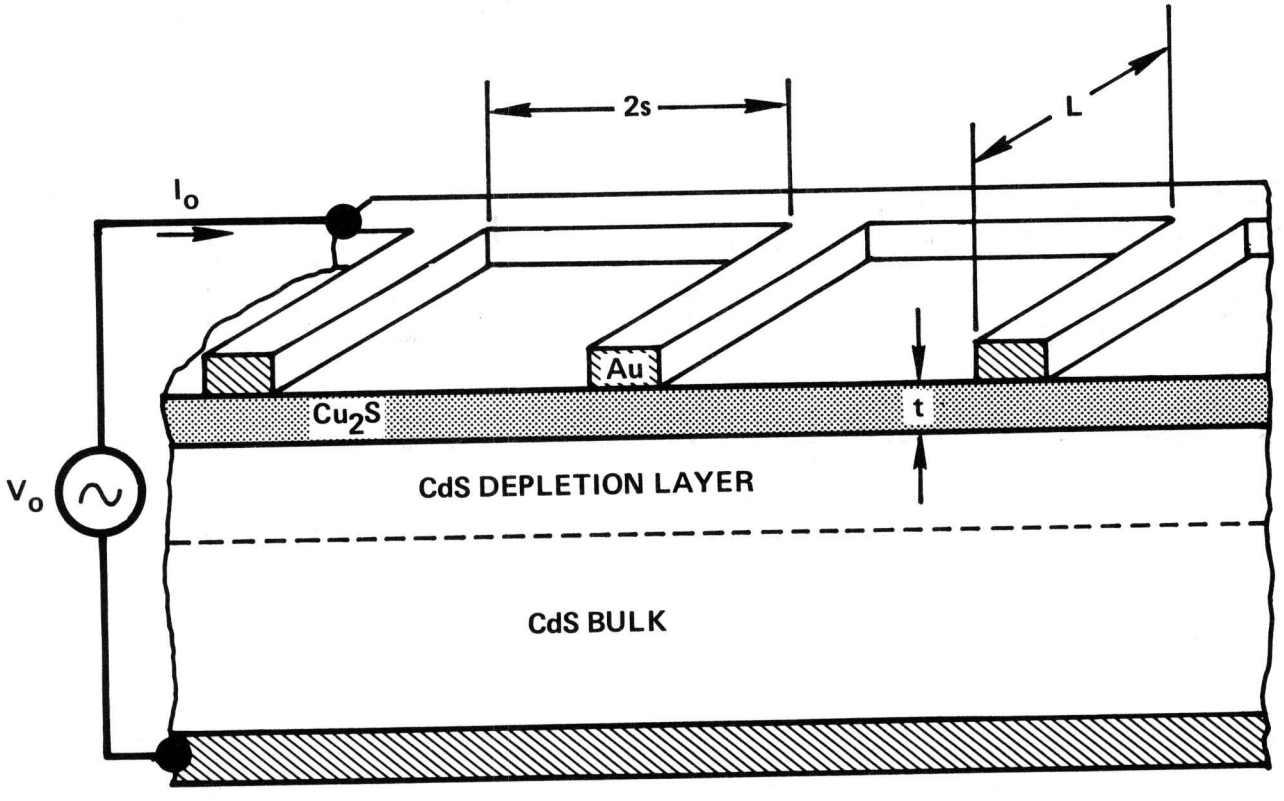

FIG. 1 Structure of Cu_2S/CdS Solar Cell.

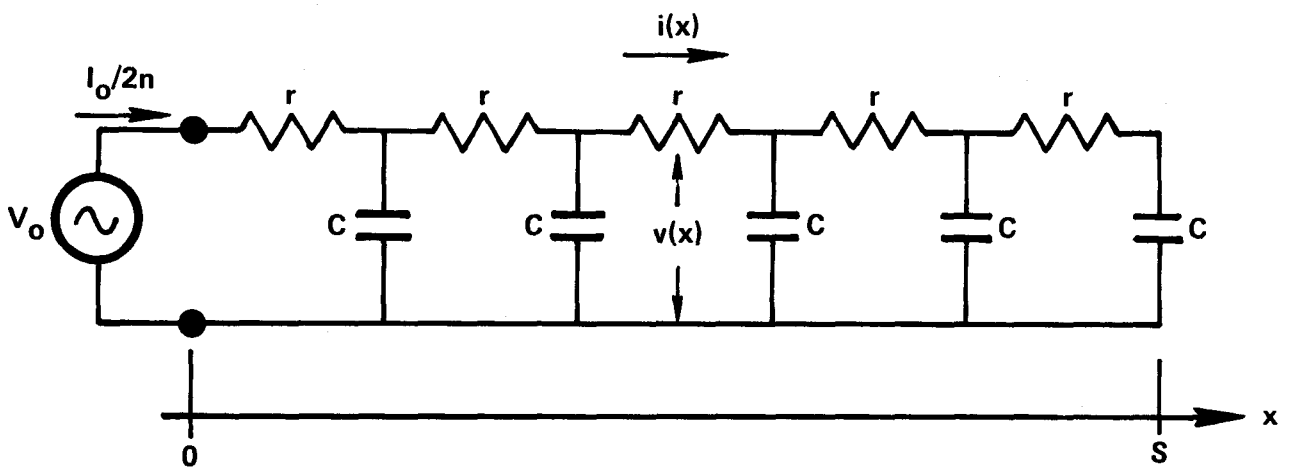

FIG. 2 Elementary section of distributed impedance of Cu_2S/CdS Solar Cell.

and

$$\frac{dv}{dx} = -ri \tag{2}$$

with solutions

$$i = \frac{I_o}{2n} \frac{\sinh\sqrt{j\omega rc}\ (s-x)}{\sinh\sqrt{j\omega rc}\ s} \tag{3}$$

and

$$v = \frac{1}{j\omega c} \frac{J_o}{2n} \sqrt{j\omega rc} \frac{\cosh\sqrt{j\omega rc}\ (s-x)}{\sinh\sqrt{j\omega rc}\ s} \quad . \tag{4}$$

The device terminal admittance is then

$$Y = j\omega C_o A \frac{\sinh(\sqrt{j\omega R_\square C_o}\ s)}{(\sqrt{j\omega R_\square C_o}\ s)\cosh(\sqrt{j\omega R_\square C_o}\ s)} \tag{5}$$

where the device area is given by $A = 2nsL$. Writing the admittance in the form

$$Y = j\omega C(\omega) + G(\omega)$$

the frequency dependence of the apparent capacitance is given by

$$C(\omega) = C_o A\ \mathrm{Re}\left[\frac{\sinh\ (\sqrt{j\omega R_\square C_o}\ s}{\sqrt{j\omega R_\square C_o}\ s\ \cosh(\sqrt{j\omega R_\square C_o}\ \ s)}\right] \tag{6}$$

and the conductance by

$$G(\omega) = \frac{A}{R_\square s^2}\ \mathrm{Re}\left[\frac{\sqrt{j\omega R_\square C_o}\ s\ \sinh(\sqrt{j\omega R_\square C_o}\ s)}{\cosh(\sqrt{j\omega R_\square C_o}\ s)}\right] \tag{7}$$

Dispersion of both C and G may be written in terms of the dimensionless variable $\Omega = \omega\ R_\square C_o s^2$. The frequency dependence of C and G is shown in the normalized curves of Fig. 3. Significant dispersion in C occurs for $\Omega \geq 1$ or $f \geq 1/(2\pi R_\square C_o s^2)$. The high and low frequency asympotic behavior is readily seen

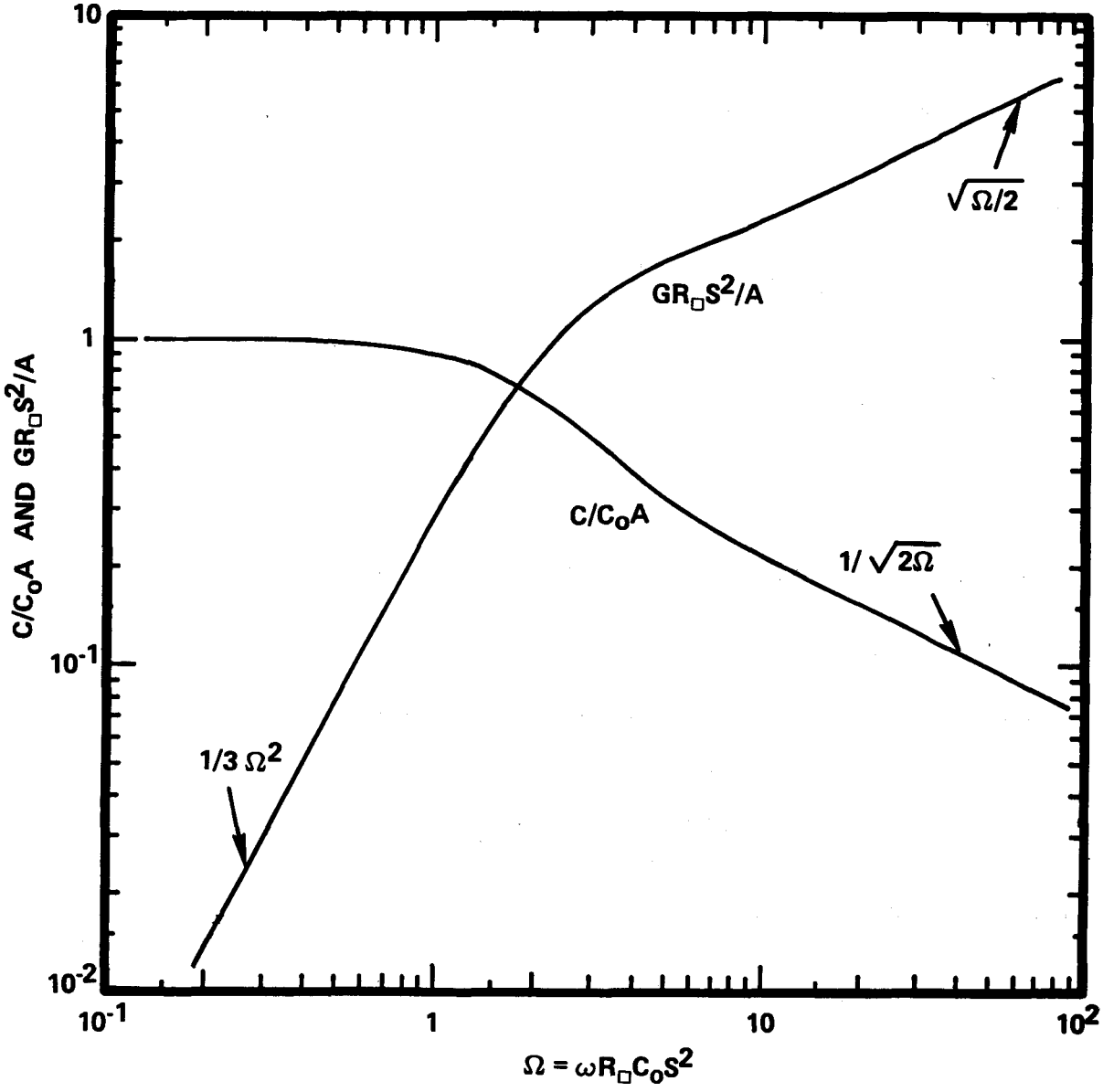

FIG. 3 Normalized C-ω and G-ω characteristics of distributed network of Figure 2.

in the 3-decade interval presented in Figure 3:

$$C/C_oA \approx 1/\sqrt{2\Omega} \quad \text{for } \Omega > 10 \tag{8a}$$

$$GR_{\square}s^2/A \approx \sqrt{\Omega/2} \quad \text{for } \Omega > 10 \tag{8b}$$

$$C/C_oA \approx 1 \quad \text{for } \Omega < 0.4 \tag{8c}$$

$$GR_{\square}s^2/A \approx \Omega^2/3 \quad \text{for } \Omega < 0.4 \tag{8d}$$

The CdS/Cu_2S cell under consideration consisted of an evaporated layer of CdS (supplied by Institute of Energy Conversion, Newark, DE) and a sputter deposited Cu_2S layer (by Telic Corp., Santa Monica, CA). The CdS layer was nominally 30 μm thick and with a resistivity of 1 to 3 Ω-cm. Prior to depositing the sputtered Cu_2S coatings, the cells were etched in a 25% (by volume) HCl solution held at 60°C for 40 sec. The etch resulted in a textured surface which prevents determination of Cu_2S thickness and resistivity as deposited on the CdS. However, Cu_2S deposited under identical conditions on a smooth surface (glass) was characterized by $\rho = 0.5\ \Omega$ - cm.

Measured C - f and G - f characteristics of the CdS/Cu_2S device in room light are shown in Figure 4. To obtain the observed frequency break point on the C vs f curve, it is necessary to assume $\rho = .68\ \Omega$ - cm rather than the $\rho = .5\ \Omega$-cm obtained on a calibration deposition. The Cu_2S layer is 0.075 μm thick. The shift in frequency breakpoint could also be due to an effective increase in Au grid separation, 2s, due to the CdS surface texturing described in the preceeding paragraph. Given C(f), G(f) is completely determined as per Equation (7). However, the cell is also characterized by a fixed shunt conductance of 6×10^{-5} S which, when added to G(f) in Equation 7, results in the calculated G(f) curve shown in Figure 4.

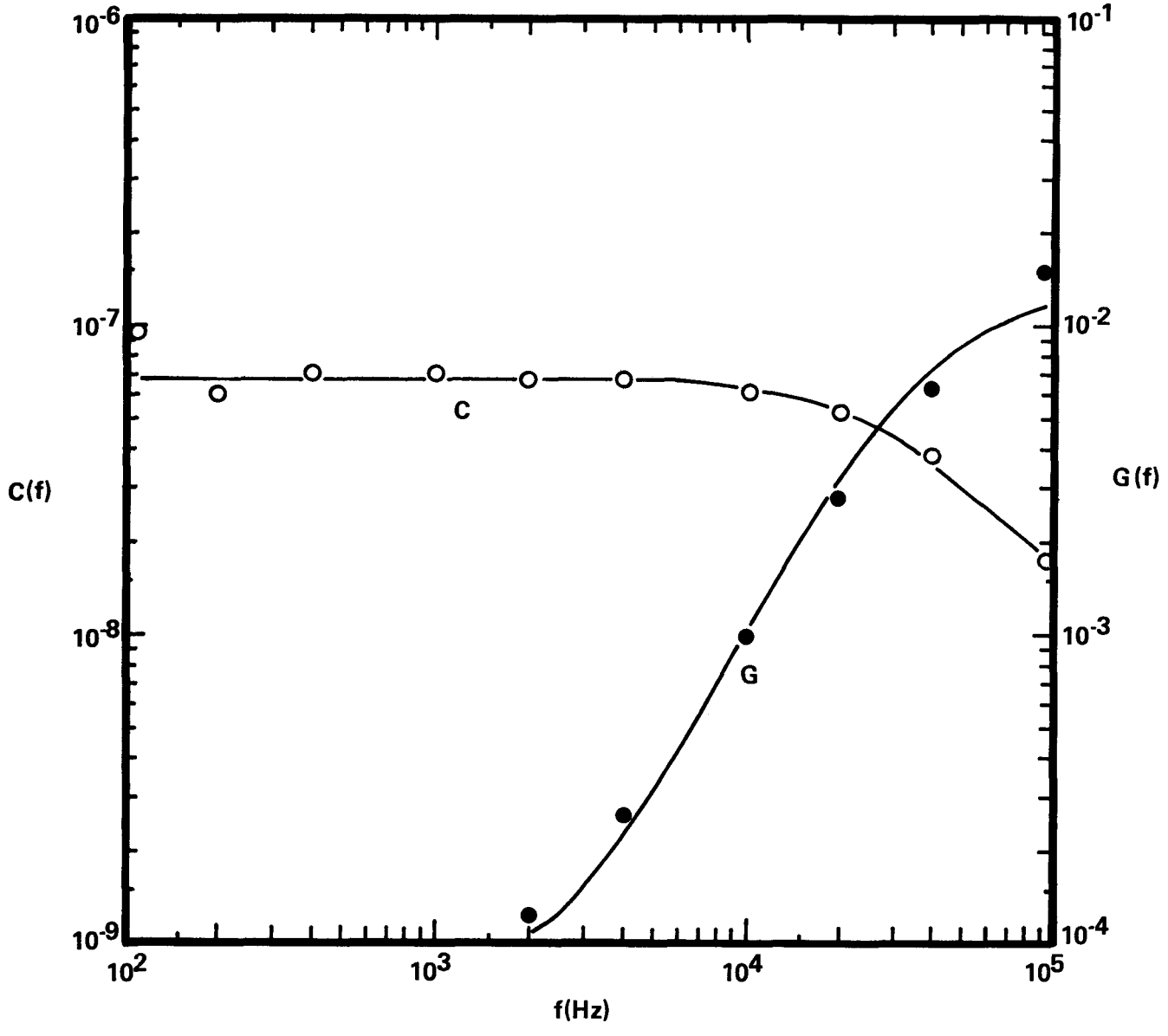

FIG. 4 Measured C-f and G-f characteristics for CdS/Cu_2S cell with thin (750Å) Cu_2S layer.

★U.S. GOVERNMENT PRINTING OFFICE: 1981-740-145/2307